arXiv:1106.1490v1 [nucl-th] 8 Jun 2011

Rotational states in deformed nuclei: An analytic approach

W. Bentz,[1, *] A. Arima,[2] J. Enders,[3] A. Richter,[3, 4] and J. Wambach[3]

[1]Department of Physics, School of Science, Tokai University,
1117 Kitakaname, Hiratsuka-shi, Kanagawa 259-1292, Japan
[2]Musashi University, 1-26-1 Toyotama-kami, Nerima-ku, Tokyo 176-8534, Japan
[3]Institut für Kernphysik, Technische Universität Darmstadt,
Schlossgartenstrasse 9, D-64289 Darmstadt, Germany
[4]ECT*, Villa Tambosi, I-38123 Villazzano (Trento), Italy

The consequences of the spontaneous breaking of rotational symmetry are investigated in a field theory model for deformed nuclei, based on simple separable interactions. The crucial role of the Ward-Takahashi identities to describe the rotational states is emphasized. We show explicitly how the rotor picture emerges from the isoscalar Goldstone modes, and how the two-rotor model emerges from the isovector scissors modes. As an application of the formalism, we discuss the M1 sum rules in deformed nuclei, and make connection to empirical information.

PACS numbers: 21.10.Ky,21.10.Re,21.60.Ev

I. INTRODUCTION

The common approach to describe deformed nuclei is based on the mean field (Hartree) approximation, where the rotational symmetry of the Hamiltonian is spontaneously broken[1, 2]. As a consequence of the broken symmetry, Goldstone poles emerge in the Bethe-Salpeter (BS) equation (or, equivalently, the RPA equation) for a particle-hole pair[3], similar to the case of infinite systems[4]. For finite systems with axial symmetry, these intrinsic zero modes lead to the picture of collective rotation of the whole system around an axis perpendicular to the symmetry axis, thereby restoring the symmetry of the original Hamiltonian[5]. The corresponding rotational band is characterized by *finite* excitation energies. The self consistency relations for the deformed mean fields[6] provide the necessary conditions for the existence of the Goldstone poles and the ground state rotational band. These features, which will be elucidated in this paper by using a simple field theory model for nucleons, were discussed transparently in models based on bosonic degrees of freedom[7], and form the basis for the construction of effective theories for deformed nuclei[8].

Besides these collective rotations of the whole system, which can be called isoscalar rotations, there exist also rotational modes of isovector character, i.e., rotational vibrations of protons against neutrons[9, 10]. These so-called scissors modes, which were predicted originally in the 2-rotor model[11] and further investigated by using sum rule methods[12] and the Interacting Boson Model[13], can be excited by the isovector orbital part of the M1 operator, and decouple automatically from the isoscalar rotational modes if the self consistency relations are satisfied [6, 14]. Recent experimental investigations[15, 16] on the scissors modes have concentrated on magnetic sum rules, which are very important because they provide the connection of the collective modes to quantities like the effective orbital g-factors or moments of inertia, which can be determined by other independent analyzes[17]. The experimental and theoretical works on the scissors modes and other magnetic dipole modes at higher excitations energies[18] are summarized in a recent extensive review[19].

The purpose of the present paper is threefold: First, we wish to elucidate the importance of the Ward-Takahashi identities[20] to describe the intrinsic isoscalar Goldstone modes and the ground state rotational band. In particular, we wish to show that the results derived for example in Ref.[6] can be obtained rather elegantly by using the Ward-Takahashi identities without explicit reference to single particle wave functions or truncations of the model space. Second, we wish to discuss how the isovector scissors mode, which corresponds to a RPA solution with finite energy, leads to the two-rotor picture in a simple model calculation. (To the best of our knowledge, a simple and direct derivation of the rotor picture from the intrinsic Goldstone modes, and of the two-rotor picture from the isovector scissors modes, has not yet been presented.) Third, we wish to investigate the inverse energy weighted and energy weighted M1 sum rules, and discuss the relation to recent experimental works on the scissors modes. For these purposes, we will use a simple field theory model based on a separable quadrupole-quadrupole (QQ) interaction in the BS (RPA) framework, and consider only the orbital motion of the nucleons. Our main interest here is the physics of the rotational modes at low energies in well deformed heavy nuclei, and there is evidence both experimentally[19] and theoretically[10] that these low energy modes are basically of orbital character.

It should be noted here that separable interactions have widely been used to investigate deformed nuclei in the RPA[21–23]. In order to perform quantitative calculations, it is well known that pairing plays an important role. The Nambu-Gorkov formalism [24] actually provides a simple way to incorporate the effects of pairing into the properties of quasiparticles. Our purpose here,

---

*Corresponding author: bentz@keyaki.cc.u-tokai.ac.jp

however, is to gain analytic insights into the physics behind the rotational states and the associated sum rules in the most simple and transparent way. Therefore, the pairing effects will not be included in the formulas, and numerical results will not be presented in this paper. Our hope is that the analytic approach described here can be extended to more general types of interactions.

In Sect. 2 we will formulate the mean field approximation and the BS equation for our model. In Sect. 3 we will use the Ward-Takahashi identities for angular momentum conservation to derive several important relations and low-energy theorems for Green functions. The connections to observables will be established in Sect. 4, where we will discuss basic properties of transition matrix elements, and in Sect. 5, where the M1 sum rules will be derived. In Sect. 6 we will discuss the derivation of the rotor picture from the isoscalar Goldstone modes, and of the 2-rotor picture from the isovector scissors modes. For the derivation of the ground state rotational band, no further approximations are necessary, but in order to derive the two-rotor picture we still find it necessary to assume a harmonic oscillator potential for the spherical part of the mean field. A summary and an outlook are given in Sect. 7.

II. THE MODEL

The Hamiltonian of the model which we will use in this paper is given by

$$\begin{aligned} H = h_{0p} + h_{0n} &+ \frac{\chi_{pp}}{2}\left(Q_p^\dagger \cdot Q_p + Q_n^\dagger \cdot Q_n\right) \\ &+ \frac{\chi_{pn}}{2}\left(Q_p^\dagger \cdot Q_n + Q_n^\dagger \cdot Q_p\right). \end{aligned} \tag{II.1}$$

Here $h_{0\tau} = \int \mathrm{d}^3x\, \psi_\tau^\dagger(x) H_0(x) \psi_\tau(x)$, where $H_0(x) = -\Delta/2M + U_0(r)$ with M the nucleon mass and $U_0(r)$ some spherical mean field. The quadrupole operator is defined by

$$Q_\tau^K = \int \mathrm{d}^3x\, \psi_\tau^\dagger(x) Q^K(x) \psi_\tau(x) \qquad (\tau = p, n), \tag{II.2}$$

where $Q^K(x) = r^2 Y_{2K}(\hat{x})$ [1], and the products $Q^\dagger \cdot Q$ in (II.1) are defined as $Q^\dagger \cdot Q \equiv \sum_{K=-2}^{2} Q^{K\dagger} Q^K$. For the coupling constants of the QQ force we assume $\chi_{nn} = \chi_{pp}$ and $\chi_{pn} = \chi_{np}$. Because we treat protons and neutrons as separate particles, the interaction in (II.1) is a mixture of pure isoscalar ($\chi_{pn} = \chi_{pp}$) and pure isovector ($\chi_{pn} = -\chi_{pp}$) type interactions.

A. Mean field approximation

The mean field approximation is formulated as usual by adding and subtracting a term $-\sum_\tau \beta_\tau Q_\tau^0 + C$ in (II.1), where the parameters β_τ and the constant C will be determined later by the requirement of self consistency. In order to avoid mathematical ambiguities in the low energy theorems to be discussed later, we also add the terms $-\sum_\tau \varepsilon_\tau Q_\tau^0$, which explicitly break the rotational symmetry. (In the final results the symmetry breaking parameters ε_τ will be set to zero[2].) In this way we obtain

$$\begin{aligned} H = H_{0p} + H_{0n} + C + \Big\{ &(\beta_p - \varepsilon_p)\, Q_p^0 + (\beta_n - \varepsilon_n)\, Q_n^0 \\ &+ \frac{\chi_{pp}}{2}\left(Q_p^\dagger \cdot Q_p + Q_n^\dagger \cdot Q_n\right) \\ &+ \frac{\chi_{pn}}{2}\left(Q_p^\dagger \cdot Q_n + Q_n^\dagger \cdot Q_p\right) - C \Big\}, \end{aligned} \tag{II.3}$$

where

$$H_{0\tau} = \int \mathrm{d}^3x\, \psi_\tau^\dagger(x) \left(-\frac{\Delta}{2M} + U_0(x) - \beta_\tau Q^0(x) \right) \psi_\tau(x). \tag{II.4}$$

We now assume that the rotational symmetry is spontaneously broken, i.e., that only the $K = 0$ component of the quadrupole operator has a finite ground state expectation value:

$$Q_\tau^0 = \langle Q_\tau^0 \rangle + :Q_\tau^0: , \tag{II.5}$$

where the dots in the second term denote normal ordering. We require that the part $\{\dots\}$ in (II.3) becomes a "true" residual interaction, i.e; when (II.5) is inserted into (II.3), this part has neither terms linear in $:Q_\tau^0:$ nor constant (c-number) terms. The first requirement leads to the self consistency relations

$$\begin{aligned} \beta_p &= \varepsilon_p - \chi_{pp}\langle Q_p^0 \rangle - \chi_{pn}\langle Q_n^0 \rangle, \\ \beta_n &= \varepsilon_n - \chi_{nn}\langle Q_n^0 \rangle - \chi_{np}\langle Q_p^0 \rangle, \end{aligned} \tag{II.6}$$

and the second requirement determines C as

$$C = -\frac{\chi_{pp}}{2}\left(\langle Q_p^0 \rangle^2 + \langle Q_n^0 \rangle^2\right) - \chi_{pn}\langle Q_p^0 \rangle \langle Q_n^0 \rangle. \tag{II.7}$$

Self consistency implies that the expectation values $\langle Q_\tau^0 \rangle$ in Eqs. (II.6) themselves depend on β_τ. The Hamiltonian finally becomes

$$H = H_{0p} + H_{0n} + C + \sum_{\tau\rho} \frac{\chi_{\tau\rho}}{2}\left(:Q_\tau^\dagger:\right) \cdot \left(:Q_\rho:\right). \tag{II.8}$$

---

[1] For clarity, we will also use the notations $Q_p^K(x)$ or $Q_n^K(x)$ to indicate whether the quadrupole field refers to protons or neutrons. In this paper, the labels τ, ρ, λ stand for protons (p) or neutrons (n). If a sum over those labels is involved, it will be indicated explicitly.

[2] These symmetry breaking parameters ε should not be confused with the single particle energies, for which we will use the symbol ϵ.

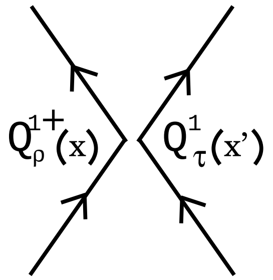

FIG. 1: Graphical representation of the particle-hole interaction kernel Eq.(II.9). In this and all following diagrams, time can be visualized to run from left to right.

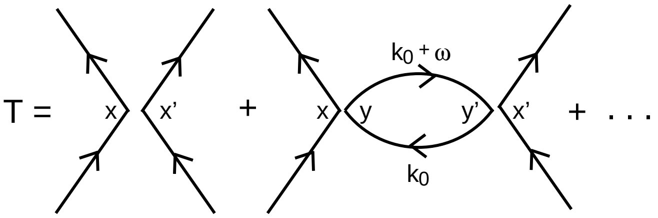

FIG. 2: Graphical representation of the particle-hole T-matrix Eq.(II.10) in the ladder approximation.

If one employs a harmonic oscillator potential $U_0(r) = \left(M\tilde{\omega}^2/2\right) r^2$, it is sometimes convenient to define dimensionless deformation parameters $\tilde{\beta}_\tau$ by $\beta_\tau = M\tilde{\omega}^2\tilde{\beta}_\tau$, because then one can express the sum $U_0(x) - \beta_\tau Q^0(x)$ in (II.4) as a deformed harmonic oscillator potential and apply standard methods of the Nilsson model[25]. Except for the last parts of this paper (Sect. 6.B), we will keep the discussions general without specifying the form of U_0.

B. Collective excitations

Here we consider the Bethe-Salpeter (BS) equation, which is equivalent to the RPA equation, for a particle and a hole in the $K = 1$ channel. [3]

The residual interaction in (II.8) is separable in coordinate space, see Fig.1. The corresponding Feynman rule for the particle-hole interaction kernel is given by

$$K_{\tau\rho}(x', x) = -iQ^1_\tau(x')\chi_{\tau\rho}Q^{1\dagger}_\rho(x). \tag{II.9}$$

The inhomogeneous BS equation then reads (see Fig.2)

$$\begin{aligned} T_{\tau\rho}(x', x; \omega) &= K_{\tau\rho}(x', x) + \int \mathrm{d}^3y' \int \mathrm{d}^3y \int \frac{\mathrm{d}k_0}{2\pi} \sum_\lambda \\ &K_{\tau\lambda}(x', y')\, S_\lambda(y', y; k_0 + \omega)\, S_\lambda(y, y'; k_0)\; T_{\lambda\rho}(y, x; \omega)\,. \end{aligned} \tag{II.10}$$

Here we work with a mixed representation of the Feynman propagator:

$$\begin{aligned} S_\tau(x', x; \omega) &= \sum_{\alpha\in\tau} \frac{\phi_{\tau\alpha}(x')\phi^\dagger_{\tau\alpha}(x)}{\omega - \epsilon_{\tau\alpha} + i\delta} + \sum_{i\in\tau} \frac{\phi_{\tau i}(x')\phi^\dagger_{\tau i}(x)}{\omega - \epsilon_{\tau i} - i\delta}, \\ &\equiv S_{\tau P} + S_{\tau H}, \end{aligned} \tag{II.11}$$

where $\phi_{\tau\alpha}(x)$ and $\epsilon_{\tau\alpha}$ are the eigenfunctions and eigenvalues of $H_{0\tau}$ for particle (P) states, and $\phi_{\tau i}(x)$, $\epsilon_{\tau i}$ denote the corresponding quantities for hole (H) states [4].

Inserting the kernel Eq.(II.9) and the ansatz

$$T_{\tau\rho}(x', x; \omega) \equiv -iQ^1_\tau(x')t_{\tau\rho}(\omega)Q^{1\dagger}_\rho(x) \tag{II.12}$$

into (II.10), we obtain the following simple matrix equation for the reduced T-matrix:

$$\begin{aligned} &t(\omega) = \chi - \chi\,\pi(\omega)\,t(\omega), \\ \Rightarrow\quad &t(\omega) = \frac{1}{1 + \chi\pi(\omega)}\,\chi = \chi\,\frac{1}{1 + \pi(\omega)\chi}. \end{aligned} \tag{II.13}$$

Here the matrices in charge space have the form

$$t = \begin{pmatrix} t_{pp} & t_{pn} \\ t_{np} & t_{nn} \end{pmatrix}, \quad \chi = \begin{pmatrix} \chi_{pp} & \chi_{pn} \\ \chi_{np} & \chi_{nn} \end{pmatrix}, \quad \pi = \begin{pmatrix} \pi_p & 0 \\ 0 & \pi_n \end{pmatrix}, \tag{II.14}$$

and the proton and neutron "bubble graphs" $\pi_\tau(\omega)$ are given by (see Fig. 3 and Appendix A)

$$\begin{aligned} \pi_\tau(\omega) &= i \int \frac{\mathrm{d}k_0}{2\pi} \int \mathrm{d}^3x \int \mathrm{d}^3x' \\ &\quad\times \left[Q^{1\dagger}_\tau(x')S_\tau(x', x; k_0 + \omega)\,Q^1_\tau(x)S_\tau(x, x'; k_0)\right], \\ &= -2 \sum_{(\alpha i)\in\tau} |\langle\alpha|Q^1_\tau|i\rangle|^2 \frac{\omega_{\alpha i}}{\omega^2 - \omega^2_{\alpha i} + i\delta}. \end{aligned} \tag{II.15}$$

Here $\omega_{\alpha i} = \epsilon_\alpha - \epsilon_i$ are the non-interacting particle-hole energies.

From (II.13), the poles of the T-matrix ($\omega^2 \equiv \omega_n^2$) are determined by the equation

$$\begin{aligned} &\mathrm{Det}\,(1 + \chi\pi(\omega))) \\ &= (1 + \pi_p(\omega)\chi_{pp})\,(1 + \pi_n(\omega)\chi_{nn}) - \chi^2_{pn}\pi_p(\omega)\pi_n(\omega), \\ &= 0. \end{aligned} \tag{II.16}$$

---

[3] The $K = -1$ channel is degenerate with the $K = 1$ channel, while the $K = 0$ and the $K = \pm 2$ channels have different energies. There is no mixing of those channels for the case of axial symmetry. We consider the collective $K = \pm 1$ states here, because they correspond to the rotational states which are of main interest in this paper.

[4] Notations like $\alpha \in \tau$ (or $i \in \tau$) indicate that the single-particle state α (or the single-hole state i) is a proton ($\tau = p$) or neutron ($\tau = n$) state. We also remark that the states i in (II.11) are actually the time-reversed of the occupied single particle states.

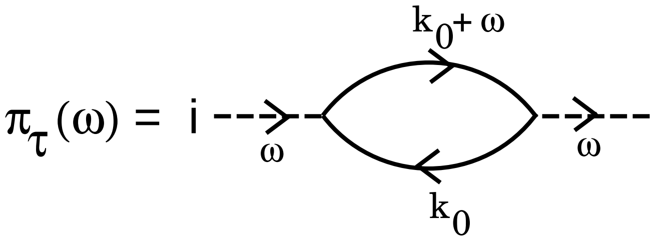

FIG. 3: Graphical representation of the bubble graph Eq.(II.15).

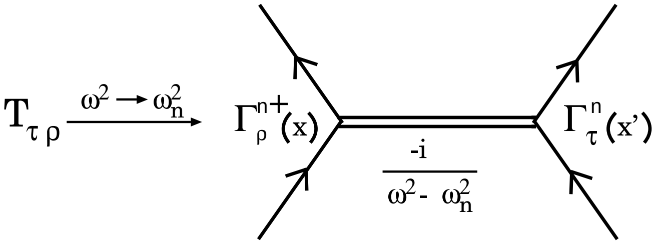

FIG. 4: Graphical representation of the pole behavior of the particle-hole T-matrix, Eq.(II.18). The double line represents a collective state.

It is straight forward to use Eq.(II.13) to determine the pole behavior of the T-matrix. The results for the reduced and the full T-matrix are (see Fig. 4 for the full T-matrix)

$$t_{\tau\rho}(\omega) \overset{\omega^2\to\omega_n^2}{\longrightarrow} \frac{N_\tau(\omega_n)N_\rho(\omega_n)}{\omega^2-\omega_n^2+i\delta}, \tag{II.17}$$

$$T_{\tau\rho}(x',x;\omega) \overset{\omega^2\to\omega_n^2}{\longrightarrow} \frac{(-i)\Gamma_\tau^n(x')\,\Gamma_\rho^{n\dagger}(x)}{\omega^2-\omega_n^2+i\delta}. \tag{II.18}$$

Here the vertex functions for the collective $K=1$ state n (excitation energy ω_n) are given by

$$\Gamma_\tau^n(x) = Q_\tau^1(x)N_\tau(\omega_n), \tag{II.19}$$

$$\Gamma_\tau^{n\dagger}(x) = Q_\tau^{1\dagger}(x)N_\tau(\omega_n), \tag{II.20}$$

with the normalization factors determined from[5]

$$\frac{1}{N_p(\omega_n)^2} = \pi_p'(\omega_n) + \pi_n'(\omega_n)\,\frac{N_n(\omega_n)^2}{N_p(\omega_n)^2}, \tag{II.21}$$

$$\frac{N_n(\omega_n)}{N_p(\omega_n)} = \frac{1+\chi_{pp}\pi_p(\omega_n)}{-\chi_{pn}\pi_n(\omega_n)} = \frac{-\chi_{pn}\pi_p(\omega_n)}{1+\chi_{nn}\pi_n(\omega_n)}. \tag{II.22}$$

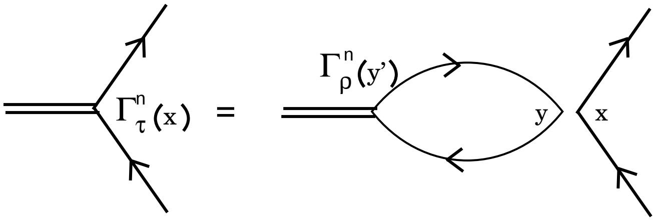

FIG. 5: Graphical representation of the homogeneous BS equation, Eq.(II.24). The double line represents a collective state.

Here the prime indicates differentiation w.r.t. ω^2, i.e.,

$$\pi_\tau'(\omega) \equiv \frac{\mathrm{d}\pi_\tau}{\mathrm{d}\omega^2} = 2\sum_{(\alpha i)\in\tau} |\langle\alpha|Q_\tau^1|i\rangle|^2 \frac{\omega_{\alpha i}}{\left(\omega^2-\omega_{\alpha i}^2+i\delta\right)^2}. \tag{II.23}$$

It is also straight forward to derive the above forms of the vertex functions (except for the overall normalization) from the homogeneous BS equation: Inserting the pole behavior (II.18) into Eq. (II.10) and taking the limit $\omega^2 \to \omega_n^2$, one obtains the homogeneous BS equation (see Fig. 5):

$$\Gamma_\tau^n(x) = -i\int \mathrm{d}^3y' \int \mathrm{d}^3y \int \frac{\mathrm{d}k_0}{2\pi} \sum_\rho \\ \times\, Q_\tau^1(x)\,\chi_{\tau\rho}\,Q_\rho^{1\dagger}(y) S_\rho(y,y';k_0+\omega) S_\rho(y',y;k_0)\,\Gamma_\rho^n(y'). \tag{II.24}$$

Inserting here the ansatz $\Gamma_\tau^n(x) = Q_\tau^1(x)N_\tau(\omega)$, one obtains the following matrix equation for the normalization factors:

$$\begin{pmatrix} N_p(\omega) \\ N_n(\omega) \end{pmatrix} = -\begin{pmatrix} \chi_{pp}\pi_p(\omega) & \chi_{pn}\pi_n(\omega) \\ \chi_{np}\pi_p(\omega) & \chi_{nn}\pi_n(\omega) \end{pmatrix} \begin{pmatrix} N_p(\omega) \\ N_n(\omega) \end{pmatrix}. \tag{II.25}$$

This equation again leads to the pole equation (II.16) with solutions $\omega = \omega_n$, and to the relation (II.22).

III. WARD-TAKAHASHI IDENTITIES

We first note the following commutation relation [26] between the angular momentum operators $L^{\pm 1} \equiv \frac{1}{\sqrt{2}}\left(L^x \pm iL^y\right)$ and a tensor operator $T_{(k)}^q$ of rank

---

[5] We normalize the vertex functions Γ as the residues at the poles in ω^2, which corresponds to "covariant normalization" in relativistic field theory. The overall sign is chosen so that for a pure isoscalar interaction ($\chi_{pp} = \chi_{pn}$) one has $N_n/N_p = 1$, and for a pure isovector interaction ($\chi_{pp} = -\chi_{pn}$) one has $N_n/N_p = -1$.

k with spherical components $q=-k\ldots k$ [6]:

$$\left[L^{\pm 1},T^{q}_{(k)}\right]=\frac{1}{\sqrt{2}}\sqrt{k(k+1)-q(q\pm 1)}\,T^{q\pm 1}_{(k)}. \tag{III.1}$$

The commutator of $H_{0\tau}$ (Eq.(II.4)) with the angular momentum operators then becomes

$$\left[H_{0\tau},L^{\pm 1}_{\tau}\right]=\sqrt{3}\beta_{\tau}Q^{\pm 1}_{\tau}, \tag{III.2}$$

and if we consider matrix elements of this identity between non-interacting particle-hole states, we obtain the useful relation

$$\langle\alpha|L^{\pm 1}_{\tau}|i\rangle=\frac{\sqrt{3}\beta_{\tau}}{\omega_{\alpha i}}\langle\alpha|Q^{\pm 1}_{\tau}|i\rangle, \tag{III.3}$$

which will be used in later Sections. (Here $(\alpha i)\in\tau$.)

Let us now discuss the Ward-Takahashi identity which follows from angular momentum conservation. We consider the time derivative of the 2-point function with external Heisenberg operators $Q^{1}_{\tau}(t')$ and $L^{1}(t)=L^{1}_{p}(t)+L^{1}_{n}(t)$. Using the Heisenberg equation of motion

$$\frac{\partial L^{1}}{\partial t}=i\left[H,L^{1}\right]=i\sqrt{3}\sum_{\tau}\varepsilon_{\tau}Q^{1}_{\tau}, \tag{III.4}$$

and the equal time commutator $\left[L^{1}(t),Q^{1\dagger}_{\tau}(t),\right]$ from (III.1), we obtain the Ward-Takahashi identity

$$\begin{aligned}&\frac{\partial}{\partial t}\langle 0|T\left(Q^{1\dagger}_{\tau}(t')\,L^{1}(t)\right)|0\rangle\\&=i\sqrt{3}\,\sum_{\lambda}\langle 0|T\left(Q^{1\dagger}_{\tau}(t')\,Q^{1}_{\lambda}(t)\right)|0\rangle\,\varepsilon_{\lambda}-\sqrt{3}\delta(t-t')\langle Q^{0}_{\tau}\rangle.\end{aligned} \tag{III.5}$$

Let us define here the *exact* 2-point functions[7] with one arbitrary operator ($K=1$ component A^{1}) and the quadrupole operator ($Q^{1\dagger}$):

$$\begin{aligned}\langle 0|T\left(Q^{1\dagger}_{\tau}(t')\,A^{1}_{\lambda}(t)\right)|0\rangle&\equiv -i\,\Pi^{QA}_{\tau\lambda}(t'-t)\\&=-i\int \mathrm{d}\omega\, e^{-i\omega(t'-t)}\Pi^{QA}_{\tau\lambda}(\omega).\end{aligned} \tag{III.6}$$

Then the Fourier transform of the Ward-Takahashi identity (III.5) can be expressed as

$$\sum_{\lambda}\omega\,\Pi^{QL}_{\tau\lambda}(\omega)=\sqrt{3}\,\sum_{\lambda}\Pi^{QQ}_{\tau\lambda}(\omega)\varepsilon_{\lambda}-\sqrt{3}\,\langle Q^{0}_{\tau}\rangle. \tag{III.7}$$

This is the basic identity which will be used in this paper. In the chain (RPA) approximation, the correlators (III.6) can be expressed in terms of the reduced particle-hole t-matrix of Eq.(II.13) as follows (see Fig. 6):

$$\Pi^{QA}_{\tau\lambda}(\omega)=\delta_{\lambda\tau}\pi^{QA}_{\tau}(\omega)-\pi_{\tau}(\omega)t_{\tau\lambda}(\omega)\pi^{QA}_{\lambda}(\omega). \tag{III.8}$$

For the case $A=Q$ one can use Eq.(II.13) to simplify this expression to

$$\Pi^{QQ}(\omega)=\frac{1}{1+\pi(\omega)\chi}\,\pi(\omega), \tag{III.9}$$

where we used the matrix notation of Eq.(II.14).

A. Identities for the Goldstone modes ($\omega\to 0$ first)

In the limit $\omega\to 0$ (but finite ε), Eq.(III.7) leads to the following low energy theorem:

$$\sum_{\lambda}\Pi^{QQ}_{\tau\lambda}(0)\,\varepsilon_{\lambda}=\langle Q^{0}_{\tau}\rangle. \tag{III.10}$$

In the RPA, the correlator $\Pi^{QQ}(\omega)$ is given by (III.9). Inserting this form into (III.10) and multiplying from left by the matrix $(1+\pi(0)\chi)$ we obtain

$$\pi(0)\left(\beta+\chi\langle Q^{0}\rangle\right)=\left(1+\pi(0)\chi\right)\langle Q^{0}\rangle,$$

where we used the self consistency relation (II.6) to eliminate ε. (In this notation, β and $\langle Q^{0}\rangle$ are considered as vectors in charge space.) We then obtain the identity

$$\pi_{\tau}(0)\beta_{\tau}=\langle Q^{0}_{\tau}\rangle, \tag{III.11}$$

which can also be shown directly by using the explicit form (II.15) of the bubble graph, see Appendix B.

Using (III.11), the self consistency relation (II.6) can be rewritten as

$$\beta_{\tau}=\varepsilon_{\tau}-\sum_{\lambda}\left(\chi_{\tau\lambda}\pi_{\lambda}(0)\right)\beta_{\lambda}. \tag{III.12}$$

In the limit of exact rotational symmetry ($\varepsilon_{\tau}=0$), this relation becomes

$$\begin{pmatrix}\beta_{p}\\ \beta_{n}\end{pmatrix}=-\begin{pmatrix}\chi_{pp}\pi_{p}(0) & \chi_{pn}\pi_{n}(0)\\ \chi_{np}\pi_{p}(0) & \chi_{nn}\pi_{n}(0)\end{pmatrix}\begin{pmatrix}\beta_{p}\\ \beta_{n}\end{pmatrix}. \tag{III.13}$$

This equation leads to the condition $\mathrm{Det}\left(1+\chi\pi(0)\right)=0$ for a nontrivial solution. Comparing this with the pole equation (II.16), we see that in the limit of exact rotational symmetry the self consistency relation guarantees the existence of a Goldstone pole ($\omega_{0}=0$) in the $K=1$ channel.

Let us now determine the vertex function for the Goldstone modes. From (II.25) and (III.13) we obtain the relation

$$\frac{N_{p}(0)}{N_{n}(0)}=\frac{\beta_{p}}{\beta_{n}}. \tag{III.14}$$

---

[6] The definition used here for the spherical components of the angular momentum ($L^{\pm 1}=(L^{x}\pm iL^{y})/\sqrt{2}$) differs in sign for the $+1$ component of any other vector ($a^{1}=-(a^{x}+ia^{y})/\sqrt{2}$, $a^{-1}=(a^{x}-ia^{y})/\sqrt{2}$). Therefore, for the case $T_{(1)}=L$ in (III.1), we have to use $T^{\pm 1}_{(1)}=\mp L^{\pm 1}$ to get the correct commutation relation $\left[L^{1},L^{-1}\right]=L^{0}=L^{z}$.

[7] We use the symbol $\Pi_{\lambda\tau}$ for the exact correlators and the correlators in the chain (RPA) approximation, and $\pi_{\lambda\tau}=\delta_{\lambda\tau}\pi_{\tau}$ for the non-interacting ones. Note that $\pi^{QQ}(\omega)=\pi(\omega)$ is the bubble graph of the previous Section.

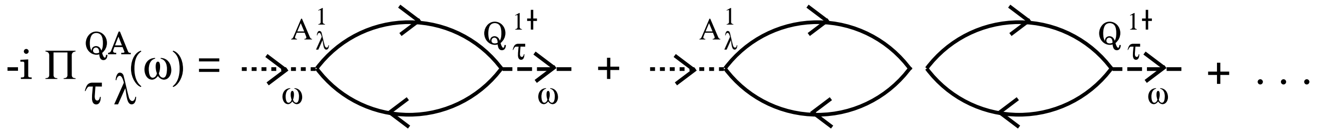

FIG. 6: Graphical representation of the 2-point function $\Pi^{QA}_{\tau\lambda}$, Eq.(III.8).

Therefore the vertex function (II.19) for the $K=1$ Goldstone mode ($n=0$) can be expressed as

$$\Gamma^{n=0}_\tau(x) = N\, Q^1_\tau(x)\beta_\tau, \tag{III.15}$$

where (see (III.14) and (II.21))

$$N_\tau(0) \equiv N\beta_\tau, \qquad \frac{1}{N^2} = \sum_\tau \beta_\tau^2 \pi'_\tau(0). \tag{III.16}$$

The derivatives of the bubble graphs at $\omega = 0$ are obtained from (II.23) and (III.3) as follows:

$$\pi'_\tau(0) = 2\sum_{(\alpha i)\in\tau} \frac{|\langle\alpha|Q^1_\tau|i\rangle|^2}{\omega^3_{\alpha i}} = \frac{2}{3\beta_\tau^2}\sum_{(\alpha i)\in\tau}\frac{|\langle\alpha|L^1_\tau|i\rangle|^2}{\omega_{\alpha i}} \tag{III.17}$$

Comparing this with the Inglis formula for the proton and neutron moments of inertia [27]

$$I_\tau = 2\sum_{(\alpha i)\in\tau}\frac{|\langle\alpha|L^1_\tau|i\rangle|^2}{\omega_{\alpha i}}, \tag{III.18}$$

we obtain the following important relations:

$$\beta_\tau^2\pi'_\tau(0) = \frac{I_\tau}{3}, \qquad N = \sqrt{\frac{3}{I}}, \qquad N_\tau(0) = \sqrt{\frac{3}{I}}\,\beta_\tau, \tag{III.19}$$

where $I = I_p + I_n$ is the total moment of inertia. The Goldstone vertex function (III.15) then takes the form

$$\Gamma^{n=0}_\tau(x) = \sqrt{\frac{3}{I}}\, Q^1_\tau(x)\beta_\tau. \tag{III.20}$$

The vertex function for the $K=-1$ Goldstone mode is obtained from (III.20) by replacing $Q^1 \to Q^{-1}$. It is easy to confirm that the sum or difference of the $K=\pm1$ vertex functions represents the change of the deformed mean field ($U_\tau(x) = U_0(x) - \beta_\tau Q^0_\tau(x)$ in the Hamiltonian (II.4)) under an infinitesimal rotation around the x or y axes [4].

B. Identities for the $Q-L$ correlator ($\varepsilon \to 0$ first)

For exact symmetry ($\varepsilon_\tau = 0$), the Ward-Takahashi identity (III.7) becomes

$$\omega\sum_\lambda \Pi^{QL}_{\tau\lambda}(\omega) = -\sqrt{3}\,\langle Q^0_\tau\rangle. \tag{III.21}$$

In the limit $\omega^2 \to \omega_n^2$, where $\omega_n \neq 0$ is one of the nonzero solutions of the eigenvalue equation (II.16), the identity (III.21) gives

$$\lim_{\omega^2\to\omega_n^2}\left(\omega^2-\omega_n^2\right)\sum_\lambda \Pi^{QL}_{\tau\lambda}(\omega) = 0 \qquad (\omega_n \neq 0). \tag{III.22}$$

Inserting here the RPA form (III.8) and using the pole behavior of the reduced T-matrix (II.17), we obtain

$$\sum_\lambda N_\lambda(\omega_n)\,\pi^{QL}_\lambda(\omega_n) = 0 \qquad (\omega_n \neq 0). \tag{III.23}$$

It is straight forward to check the validity of this relation by using the explicit form of the bubble graph π^{QL}_τ (see Appendix B).

Next, let us consider the limit $\omega \to 0$ of (III.21). For this purpose, we have to isolate the Goldstone pole on the l.h.s. Inserting the RPA form (III.8) of the correlator Π^{QL}, and isolating the Goldstone pole by using (II.17), i.e.,

$$t_{\lambda'\lambda} = \frac{N_{\lambda'}(0)N_\lambda(0)}{\omega^2} + (\text{terms regular for } \omega\to 0)\,, \tag{III.24}$$

the identity (III.21) in the limit $\omega \to 0$ becomes

$$\lim\nolimits_{\omega\to0}\sum_\lambda \pi_\tau(0)\,N_\tau(0)\,N_\lambda(0)\left(\frac{\pi^{QL}_\lambda(\omega)}{\omega}\right) = \sqrt{3}\,\langle Q^0_\tau\rangle. \tag{III.25}$$

Using here (III.11) and (III.16), we obtain

$$\lim\nolimits_{\omega\to0}\sum_\lambda\left(\frac{\pi^{QL}_\lambda(\omega)}{\omega}\right)\beta_\lambda = \frac{I}{\sqrt{3}}. \tag{III.26}$$

Again, it is easy to check this relation by using the explicit form of the bubble graph π^{QL}_λ and the Inglis formula, see Appendix B. Actually, because both sides of (III.26) are one-loop quantities which consist of proton and neutron pieces, the identity (III.26) holds for separately for protons and neutrons:

$$\lim\nolimits_{\omega\to0}\left(\frac{\pi^{QL}_\lambda(\omega)}{\omega}\right)\beta_\lambda = \frac{I_\lambda}{\sqrt{3}}. \tag{III.27}$$

The identities (III.23) and (III.27) will be useful for the discussion of transition matrix elements in the following Section.

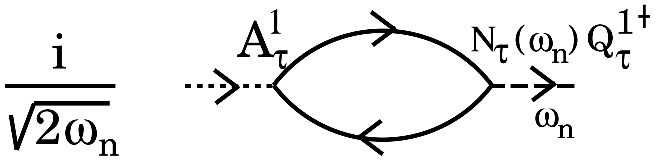
$\frac{i}{\sqrt{2\omega_n}}$
A^1_τ
$N_\tau(\omega_n)\, Q^{1\dagger}_\tau$
ω_n

FIG. 7: Graphical representation of the transition matrix element, Eq.(IV.1).

IV. TRANSITION MATRIX ELEMENTS

We first show that in the BS (RPA) framework the transition matrix element of the $K = 1$ component of any tensor operator A^1_τ from the ground state to an excited state (excitation energy ω_n and $K = 1$) is given by (see Fig. 7)

$$\langle \omega_n, K = 1|A^1_\tau|0\rangle = \frac{1}{\sqrt{2\omega_n}} \pi^{QA}_\tau(\omega_n)\, N_\tau(\omega_n). \qquad \text{(IV.1)}$$

This formula reduces the determination of the summed transition strength

$$B\,(A_\tau; K = 0 \to |K| = 1) = 2\sum_n |\langle \omega_n, K = 1|A^1_\tau|0\rangle|^2 \qquad \text{(IV.2)}$$

to a straight forward calculation of the Feynman diagram of Fig.7. (The factor 2 comes from the contribution of $K = -1$.)

To show (IV.1), we use the spectral representation of the exact correlator (III.6):

$$\begin{aligned}&\Pi^{QA}_{\tau\lambda}(\omega)\\ &\quad = -\sum_n \left[\frac{\langle 0|Q^{1\dagger}_\tau|n\rangle\langle n|A^1_\lambda|0\rangle}{\omega - \Omega_n + i\delta} - \frac{\langle n|Q^{1\dagger}_\tau|0\rangle\langle 0|A^1_\lambda|n\rangle}{\omega + \Omega_n - i\delta}\right].\end{aligned} \qquad \text{(IV.3)}$$

Here Ω_n are the exact excitation energies of the eigenstates $|n\rangle \equiv |\Omega_n; K = 1\rangle$ of the Hamiltonian H. We then obtain for $\Omega_n > 0$

$$\lim_{\omega\to\Omega_n} \left(\omega^2 - \Omega_n^2\right) \Pi^{QA}_{\tau\lambda}(\omega) = -2\Omega_n \langle 0|Q^{1\dagger}_\tau|n\rangle\langle n|A^1_\lambda|0\rangle. \qquad \text{(IV.4)}$$

On the other hand, in the RPA we have from (III.8) and the pole behavior of the t-matrix (II.17)

$$\begin{aligned}&\lim_{\omega\to\omega_n} \left(\omega^2 - \omega_n^2\right) \Pi^{QA}_{\tau\lambda}(\omega)\\ &\qquad\qquad = -\pi_\tau(\omega_n) N_\tau(\omega_n) N_\lambda(\omega_n) \pi^{QA}_\lambda(\omega_n).\end{aligned} \qquad \text{(IV.5)}$$

By comparing the r.h.s. of (IV.4) in the RPA ($\Omega_n = \omega_n$) with the r.h.s. of (IV.5), and noting that both expressions hold also for $A = Q$ (where $\pi^{QQ}_\lambda = \pi_\lambda$), we immediately arrive at (IV.1).

For the case $A = L = L_p + L_n$, the identity (III.23) confirms that the total angular momentum operator cannot excite a state with finite excitation energy:

$$\langle \omega_n, K = 1|L^1|0\rangle = 0 \qquad (\omega_n \neq 0). \qquad \text{(IV.6)}$$

In fact, the state $L^1|0\rangle$ has zero excitation energy because of $\left[H, L^1\right] = 0$, and (IV.6) confirms that this state is orthogonal to all states with finite excitation energy.

For the transition matrix element (IV.1) of the operator L_τ to the Goldstone mode, we can use the form of $N_\tau(0)$ from (III.19) and the identity (III.27) to obtain

$$\langle \omega_0, K = 1|L^1_\tau|0\rangle = \sqrt{\frac{\omega_0}{2I}}\, I_\tau \qquad (\omega_0 \to 0)\,. \qquad \text{(IV.7)}$$

If we sum over protons and neutrons, we obtain an identity which follows also directly from angular momentum conservation, Eq. (III.26):

$$\langle \omega_0, K = 1|L^1|0\rangle = \sqrt{\frac{\omega_0\, I}{2}} \qquad (\omega_0 \to 0). \qquad \text{(IV.8)}$$

This relation shows that the state $L^1|0\rangle$ is orthogonal to all RPA states, *including* the Goldstone mode. Actually, we will see in Sect. 6.A that Eq.(IV.8) is nothing but the normalization of the Goldstone state vectors.

V. M1 SUM RULES

As an application of the above formalism, we consider the inverse energy weighted (IEW) and energy weighted (EW) sum rules for the $K = 1$ component of the orbital magnetic moment (M1) operator[8]

$$M^1 = g_{\ell p}\, L^1_p + g_{\ell n}\, L^1_n, \qquad \text{(V.1)}$$

where $g_{\ell\tau}$ are the orbital g-factors for $\tau = p, n$. (The free nucleon values are $g^{\text{free}}_{\ell p} = 1,\ g^{\text{free}}_{\ell n} = 0$.)

If we define the exact 2-point function with external M1 operators by

$$\begin{aligned}\Pi^{\text{MM}}(\omega) &= i\int \mathrm{d}\tau\, e^{i\omega\tau} \langle 0|T\left(M^{1\dagger}(t')\, M^1(t)\right)|0\rangle,\\ &= -2\sum_n |\langle n|M^1|0\rangle|^2\, \frac{\Omega_n}{\omega^2 - \Omega_n^2 + i\delta},\end{aligned} \qquad \text{(V.2)}$$

where $\tau = t' - t$ and we use the notations of Eq.(IV.3) for the state vectors and energies, the IEW and EW sum rules can be expressed as follows[17] [9] :

---

[8] Generally [19], a factor $\sqrt{3/(4\pi)}$ is included in the definition of the M1 operator. This factor is not included in our definition.

$$S_{\rm IEW} \equiv 2 \sum_{\Omega_n>0} \frac{|\langle n|M^1|0\rangle|^2}{\Omega_n} = \lim_{\omega\to 0} \Pi^{MM}(\omega), \qquad \text{(V.3)}$$

$$S_{\rm EW} \equiv 2 \sum_{\Omega_n} |\langle n|M^1|0\rangle|^2 \, \Omega_n = - \lim_{\omega\to\infty} \omega^2 \, \Pi^{MM}(\omega). \qquad \text{(V.4)}$$

To evaluate these sum rules in our BS (RPA) formalism, we introduce the correlator $\Pi^{\rm LL}_{\tau\lambda}(\omega)$, which has external operators $L^{1\dagger}_\tau$ and L^1_λ. The form of $\Pi^{\rm LL}_{\tau\lambda}(\omega)$ in the RPA is (cf. Eq.(III.8))

$$\Pi^{LL}_{\tau\lambda}(\omega) = \delta_{\tau\lambda}\pi^{LL}_\tau(\omega) - \pi^{LQ}_\tau(\omega) t_{\tau\lambda}(\omega) \pi^{QL}_\lambda(\omega). \qquad \text{(V.5)}$$

Here the first term on the r.h.s. is the non-interacting bubble graph. (For the explicit form, see Eq.(A.6).)

Concentrating first on the IEW sum rule, we note from the Inglis formula (III.18) that $\pi^{LL}_\tau(0)$ is identical to the moment of inertia:

$$\pi^{LL}_\tau(\omega=0) = 2 \sum_{(\alpha i)\in\tau} \frac{|\langle\alpha|L^1_\tau|i\rangle|^2}{\omega_{\alpha i}} = I_\tau. \qquad \text{(V.6)}$$

To evaluate the second term in (V.5) in the limit $\omega \to 0$, we use the relation (III.27), which shows that only the first (singular) term in the reduced T-matrix of Eq.(III.24) contributes. Using the form of the normalization factors given in (III.19), we obtain

$$\lim_{\omega\to 0} \pi^{LQ}_\tau(\omega) t_{\tau\lambda}(\omega) \pi^{QL}_\lambda(\omega) = \frac{I_\tau I_\lambda}{I}. \qquad \text{(V.7)}$$

The LL-correlator (V.5) for $\omega \to 0$ is then obtained as

$$\lim_{\omega\to 0} \Pi^{LL}_{\tau\lambda}(\omega) = \delta_{\tau\lambda} I_\tau - \frac{I_\tau I_\lambda}{I}. \qquad \text{(V.8)}$$

This result shows that the sum rule vanishes for the case where one of the external operators is the total angular momentum L, i.e.,

$$\lim_{\omega\to 0} \sum_\lambda \Pi^{LL}_{\tau\lambda}(\omega) = 0. \qquad \text{(V.9)}$$

This is one of the many cases where the RPA-type correlations completely cancel the non-interacting (mean field) contribution, so as to satisfy the conservation laws (angular momentum conservation in the present case).

Using (V.8), we obtain for the IEW sum rule (V.3)

$$S_{\rm IEW} = \lim_{\omega\to 0} \sum_{\tau\lambda} g_{\ell\tau} \Pi^{LL}_{\tau\lambda}(\omega) g_{\ell\lambda} = \frac{4 I_p I_n}{I} \left(g_{\ell,IV}\right)^2, \qquad \text{(V.10)}$$

where we define the isovector orbital g-factor by

$$g_{\ell,IV} = \frac{1}{2}\left(g_{\ell p} - g_{\ell n}\right). \qquad \text{(V.11)}$$

Before we continue to discuss the EW sum rule, we note the following two points: First, one can separate a term proportional to $L^1 = L^1_p + L^1_n$ in the magnetic moment operator (V.1) according to

$$M^1 = \alpha \, L^1 + \left(g_{\ell,p} - \alpha\right) L^1_p + \left(g_{\ell,n} - \alpha\right) L^1_n, \qquad \text{(V.12)}$$

where α is any number. (The choice $\alpha = \frac{1}{2}$ leads to the conventional separation into isoscalar and isovector parts.) From the result (V.9) it is clear that the first term in (V.12) does not contribute to the sum rule, and the contribution of the second term is independent of α and given by (V.10). It is possible to choose α so that the RPA-type contributions vanish and the total result is given by the non-interacting correlator. This choice is

$$\alpha = \frac{I_p}{I} \, g_{\ell p} + \frac{I_n}{I} \, g_{\ell n} \equiv g_{\ell,IS}, \qquad \text{(V.13)}$$

which leads to the following separation of the magnetic moment operator into "isoscalar" and "isovector" pieces:

$$M^1 = g_{\ell,IS} \, L^1 + g_{\ell,IV} \left(\frac{2I_n}{I} L^1_p - \frac{2I_p}{I} L^1_n \right). \qquad \text{(V.14)}$$

Both the IEW and EW sum rules discussed in this Section emerge exclusively from the second (isovector) part of Eq.(V.14). We will see in Sect. 6 that this way to split the M1 operator follows naturally if one performs a minimal substitution in the effective Hamiltonians for the isoscalar (Goldstone) and isovector (scissors) rotational modes separately.

Second, the IEW sum rule for the operator $(2I_n/I)L^1_p - (2I_p/I)L^1_n$ is often interpreted as the collective mass parameter of the isovector rotation[12]. The result (V.10) then confirms that this mass parameter is given by the "isovector moment of inertia", which is defined as

$$I_{\rm IV} = \frac{4 I_p I_n}{I}. \qquad \text{(V.15)}$$

Turning now to the EW sum rule (V.4), we note that for the first term in the correlator (V.5) we have

$$- \lim_{\omega\to\infty} \omega^2 \pi^{LL}_\tau(\omega) = 2 \sum_{(\alpha i)\in\tau} \omega_{\alpha i} |\langle\alpha|L^1_\tau|i\rangle|^2, \\ = 3\beta^2_\tau \pi_\tau(0) = 3\beta_\tau \langle Q^0_\tau\rangle, \qquad \text{(V.16)}$$

where in the second equality we used the relation (III.3) to express the result in terms of the bubble graph $\pi_\tau(0)$, and in the last equality we used the low energy theorem (III.11). To evaluate the second term in the RPA correlator (V.5) in the limit $\omega \to \infty$, we note that in this limit the t-matrix (II.13) becomes simply the 4-Fermi interaction constant χ. Using also the form of the mixed bubble graph $\pi_\tau^{LQ}(\omega)$ given in (A.5) and the identity (III.3), we obtain

---

[9] The factor 2 in these expressions counts for the contribution from the $K=-1$ component M^{-1}. (Equivalently, one can express the sum rules by M^x or M^y.) We also note that, at least in the RPA (see Eq.(IV.7)), the Goldstone term does not contribute to the spectral sum in (V.2) for finite ω, and therefore also not in the $\omega \to 0$ limit of Eq.(V.3).

$$\begin{aligned}&\lim_{\omega\to\infty} \omega^2 \pi_\tau^{LQ}(\omega) t_{\tau\lambda}(\omega) \pi_\lambda^{QL}(\omega)\\ &= 3\left(\beta_\tau \pi_\tau(0)\right) \chi_{\tau\lambda} \left(\beta_\lambda \pi_\lambda(0)\right) = 3\langle Q_\tau^0\rangle \chi_{\tau\lambda} \langle Q_\lambda^0\rangle. \qquad \text{(V.17)}\end{aligned}$$

Adding the pieces (V.16) and (V.17) we obtain

$$\begin{aligned}&-\lim_{\omega\to\infty} \omega^2 \Pi_{\tau\lambda}^{LL}(\omega)\\ &\qquad = 3\left(\langle Q_\tau^0\rangle \beta_\tau \delta_{\tau\lambda} + \langle Q_\tau^0\rangle \chi_{\tau\lambda} \langle Q_\lambda^0\rangle\right). \qquad \text{(V.18)}\end{aligned}$$

Because of the self consistency relation (II.6) for exact rotational symmetry ($\varepsilon_\tau = 0$), we confirm that the expression (V.18) vanishes if we sum over τ or λ, which is again a consequence of angular momentum conservation. In order to get the EW sum rule for the M1 operator, we can therefore discard the first term in (V.14). By using again the relations (II.6) we finally obtain the following result:

$$\begin{aligned}S_{\rm EW} &= -\lim_{\omega\to\infty} \omega^2 \sum_{\tau,\lambda} g_{\ell,\tau} \Pi_{\tau\lambda}^{LL}(\omega) g_{\ell,\lambda},\\ &= -12\left(g_{\ell,IV}\right)^2 \langle Q_p^0\rangle \chi_{pn} \langle Q_n^0\rangle. \qquad \text{(V.19)}\end{aligned}$$

This is essentially the result which has been obtained in Ref.[14] by an explicit calculation of the corresponding double commutator. We also wish to mention that the EW sum rule for the operator $(2I_n/I)L_p^1 - (2I_p/I)L_n^1$ is often interpreted physically in terms of the restoring potential energy of the isovector rotation[12]. We will see in Sect.6, however, that such an intuitive result for the restoring potential energy does not seem to emerge in our present BS (RPA) framework.

Before we discuss the connection of these sum rules to observations, we make a comment on the orbital g-factors: In a more general approach, for example the Landau-Migdal theory [28], the correlator (V.2) is represented by the Feynman diagram in the first line of Fig.8. The RPA-type correlations in the Landau-Migdal approach are included via the integral equation for the total vertex, shown in the second line of Fig.8. The driving term involves not the free but an effective magnetic moment operator, which includes all processes (tensor correlations, meson exchange currents, etc) which are not taken into account by the RPA-type correlations. To a good approximation, this effective operator can again be represented in the state-independent form (V.1), but now with effective orbital g-factors, which are different from the free ones. Therefore, in an RPA approach like our present one, the isovector g-factor in the sum rules (V.10) and (V.19) should be considered as an effective quantity, which is determined by data for magnetic moments of neighboring odd-A nuclei. It is well known[29] that this effective isovector g-factor $g_{\ell,IV}$ is larger than the free nucleon value (which is 0.5) by approximately 10%.

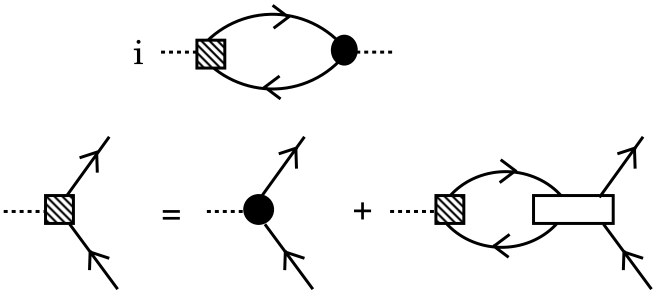

FIG. 8: Upper diagram: General representation of the correlator Eq.(V.2). The black circle represents the effective irreducible particle-hole vertex, and the shaded square represents the full particle-hole vertex including the RPA-type correlations. Lower diagrams: Graphical representation of the BS equation for the full particle-hole vertex. The open square represents the irreducible particle-hole interaction.

Let us now discuss the connection to observations: First, the 2^+ state of the ground state rotational band is a classical example of an isoscalar type rotation. (Actually, in Sect.6 we will see how it emerges from the effective Hamiltonian for the isoscalar rotational mode.) Its magnetic moment is determined only by the first term in (V.14) [30], i.e., $\mu(2^+) = g_{\ell,IS}\, L$ with $L = 2$. Its g-factor is therefore given by

$$g(2^+) = g_{\ell,IS} = \frac{I_p}{I}\, g_p + \frac{I_n}{I}\, g_n. \qquad \text{(V.20)}$$

As a first estimate one can assume that $I_p/I \simeq Z/A$ and $I_n/I \simeq N/A$, which gives

$$g_{\ell,IS} \simeq \frac{Z}{A}\, g_{\ell,p} + \frac{N}{A} g_{\ell,n} = \frac{Z}{A}, \qquad \text{(V.21)}$$

where the second equality has been derived rigorously from gauge invariance in a nuclear matter picture in Ref.[31]. We therefore obtain the familiar rotor value[2] $g(2^+) = \dfrac{Z}{A}$. For example, the nuclei considered in the analysis of Ref.[15] have $Z/A \simeq 0.4$, and the measured g-factors are $g(2^+) \simeq 0.3$. To account for the difference, one has to take into account the effects of pairing, which enhance the neutron moment of inertia relative to the proton one[32], but qualitatively the rotor value is correct.

Second, it has been shown in Ref.[15] that the IEW sum rule value (V.10) with $I_p/I \simeq Z/A$ and $I_n/I \simeq N/A$, agrees well with the experimentally determined ratio $B(M1)/\omega(M1)$, where the transition matrix element $B(M1)$ and the excitation energy $\omega(M1)$ refer to the observed low energy scissors mode. However, this agreement is only obtained if the isovector orbital g-factor $g_{\ell,IV}$ is assumed to have the same value as the isoscalar one ($g_{\ell,IS}$). As we discussed above, however, the isovector orbital g-factor should be larger than the free nucleon value, while the isoscalar one is smaller. This seems to indicate an interesting problem which deserves further study. In particular, the effects of pairing[19] should be included in the present framework. Also, for a quantitative analysis one should extend the present model to include the effects of the nucleon spin, and investigate its role for the IEW sum rule, following for example the analysis of Ref.[14] for the EW sum rule. The effects of pairing and spin should be closely investigated before drawing conclusions on the problem of the IEW sum rule.

VI. ROTATIONAL BANDS AND SCISSORS MODE

In this Section we wish to derive the effective Hamiltonians and the state vectors for the isoscalar and isovector rotational modes. Concerning the isoscalar mode, we can apply the formalism of Sects. 2 and 3 without further approximations. For the isovector mode, however, it seems necessary to refer to the harmonic oscillator model in order to obtain analytic results.

Let us first establish the connection between our formalism, which is based on the BS equation, to the usual RPA formulation in terms of “forward” and “backward” amplitudes. This connection can easily be established if we return to Eq.(IV.1) for the transition matrix element, and insert the spectral form of the non-interacting bubble graph π_τ^{QA}, which is given by Eq. (A.1) for $B = Q$. In this way we obtain[10]

$$\begin{aligned}&\langle \omega_n, K=1 | A^1_\tau | 0 \rangle \\ &= \sum_{(\alpha i)\in\tau} \left[\left(Y^*_\tau\right)_{\alpha i}(\omega_n) \, \left(A^1_\tau\right)_{\alpha i} + \left(Z^*_\tau\right)_{\alpha i}(\omega_n) \, \left(A^1_\tau\right)_{i\alpha} \right] .\end{aligned} \tag{VI.1}$$

Here we use the notation $(\mathcal{O})_{\alpha i} = \langle \alpha | \mathcal{O} | i \rangle$ for the particle-hole matrix elements of an operator $\mathcal{O}$, and the $K = 1$ components of the RPA amplitudes are defined by

$$\left(Y_\tau\right)_{\alpha i}(\omega_n) = \frac{-1}{\sqrt{2\omega_n}} \frac{N_\tau(\omega_n)\left(Q^1_\tau\right)_{\alpha i}}{\omega_n - \omega_{\alpha i} + i\delta}, \tag{VI.2}$$

$$\left(Z_\tau\right)_{\alpha i}(\omega_n) = \frac{1}{\sqrt{2\omega_n}} \frac{N_\tau(\omega_n)\left(Q^1_\tau\right)_{i\alpha}}{\omega_n + \omega_{\alpha i} - i\delta}. \tag{VI.3}$$

We recall two results of the RPA: First, the states $|\omega_n, K=1\rangle$ can be expressed by

$$|\omega_n, K=1\rangle = \mathcal{O}^\dagger(\omega_n, K=1)|0\rangle, \tag{VI.4}$$

where $\mathcal{O} = \sum_\tau \mathcal{O}^\dagger_\tau$ with

$$\begin{aligned}&\mathcal{O}^\dagger_\tau(\omega_n, K=1) \\ &\quad = \sum_{(\alpha i)\in\tau} \left[\left(Y_\tau\right)_{\alpha i}(\omega_n) \, a^\dagger_\alpha \, a_i - \left(Z_\tau\right)_{\alpha i}(\omega_n) \, a^\dagger_i \, a_\alpha \right] .\end{aligned} \tag{VI.5}$$

Here $a^\dagger$ and a are the single particle creation and annihilation operators. Second, one can derive an effective Hamiltonian for the RPA operators $\mathcal{O}^\dagger$ and $\mathcal{O}$ by following bonsonization methods based on the path integral [4] [11], i.e., introduce $\mathcal{O}^\dagger$, $\mathcal{O}$ as auxiliary quantities into the Hamiltonian and integrate over the Fermion Grassmann variables. The resulting Fermionic determinant can then be expanded in powers of $\mathcal{O}^\dagger$ and $\mathcal{O}$. Since here we are interested only in the kinetic part of the effective rotational Hamiltonian ($K = \pm 1$ modes), we simply quote the result, which is well known [2][12] and can be motivated also by more intuitive arguments:

$$H_{\text{eff}} = E_0 + \sum_n H_{\text{eff}}(\omega_n) , \tag{VI.6}$$

where

$$\begin{aligned}H_{\text{eff}}(\omega_n) &= \frac{\omega_n}{2} \sum_{K=\pm 1} \\ &\times \left[\mathcal{O}^\dagger(\omega_n, K)\mathcal{O}(\omega_n, K) + \mathcal{O}(\omega_n, K)\mathcal{O}^\dagger(\omega_n, K) \right] .\end{aligned} \tag{VI.7}$$

A. Isoscalar rotational state

Here we derive the form of the RPA amplitudes for the Goldstone modes ($\omega_0 = 0$ and $K = \pm 1$), and determine their contribution to the effective Hamiltonian (VI.7). By using the form of $N_\tau(0)$ from (III.19) and the relation (III.3), we find for the amplitudes Y and Z of (VI.2) and (VI.3):

$$\left(Y_\tau\right)_{\alpha i}(\omega_0) = \frac{\langle \alpha | L^1_\tau | i \rangle}{\sqrt{2\omega_0 I}}, \tag{VI.8}$$

$$\left(Z_\tau\right)_{\alpha i}(\omega_0) = -\frac{\langle i | L^1_\tau | \alpha \rangle}{\sqrt{2\omega_0 I}}. \tag{VI.9}$$

---

[10] We follow the notations of Ref.[1], see in particular Eqs. (14.17), (14.26) and (14.32) of Ref.[1].

[11] Bosonization methods in the path integral formalism have been used in relativistic field theories to show the equivalence of 4-Fermi type interactions to Yukawa type interactions [34], and also in nuclear structure physics to motivate the Interacting Boson Model[35].

[12] See Eq.(8.92) or (8.97) of Ref.[2]. The constant E_0 in (VI.6) corresponds to $E_{HF} - \frac{1}{2}\text{Tr}A$ in the notation of Ref.[2].

Inserting these forms into (VI.5), we obtain the representation of the Goldstone state vector as follows:

$$|\omega_0, K=1\rangle = \mathcal{O}^{+}(\omega_0, K=1)|0\rangle, \quad \text{where}$$
$$\mathcal{O}^{\dagger}(\omega_0, K=1) = \frac{L^1}{\sqrt{2\omega_0 I}}. \qquad \text{(VI.10)}$$

The creation operator for the second Goldstone mode ($K=-1$) is obtained by the replacement $L^1 \to L^{-1}$.

We see that the creation operator for the Goldstone mode diverges as $1/\sqrt{\omega_0}$ in the limit $\omega_0 \to 0$. The normalization of the Goldstone state vectors, however, is finite, and obtained from (IV.8) and (VI.10) as

$$\sum_{K=\pm 1} \langle \omega_0, K | \omega_0, K\rangle = 1. \qquad \text{(VI.11)}$$

Inserting (VI.10) into the effective Hamiltonian (VI.7), we obtain for the contribution of the Goldstone modes to the effective Hamiltonian:

$$H_{\text{eff}}(\omega_0) \equiv H_{\text{rot}}(\omega_0) = \frac{(L^x)^2 + (L^y)^2}{2I} = \frac{\vec{L}^2 - (L^3)^2}{2I}. \qquad \text{(VI.12)}$$

Because this result was derived from the intrinsic Goldstone modes, which are degenerate with the ground state of the spontaneously broken rotational symmetry, it corresponds to the ground state rotational band. The point to note is that, while the Goldstone modes have zero intrinsic excitation energy and correspond to the solution $\omega_0 = 0$ of the BS equation, the operators $\mathcal{O}^{\dagger}(\omega_0)$ and $\mathcal{O}(\omega_0)$ diverge as $1/\sqrt{\omega_0}$, and as a result the contribution of the Goldstone modes to the effective Hamiltonian (VI.7) is finite and given by the collective rotational energy (VI.12). In a microscopic quantum theory of finite systems, the Goldstone modes are therefore by no means "spurious", but describe the rotation of the whole system around an axis perpendicular to the symmetry axis, with *finite* rotational energy. Only if one *assumes* the rotational part (VI.12) from the outset, the Goldstone modes should be considered as "spurious".

B. Isovector rotational state (Scissors mode)

Contrary to the isoscalar rotational modes discussed in the previous Subsection, it seems necessary to make more specific model assumptions in order to derive the corresponding expressions for the isovector rotational modes. Here we will assume the harmonic oscillator (h.o.) form $U_0(x) = \left(M\tilde{\omega}^2/2\right) r^2$ in the mean field Hamiltonian (II.4). The sum $U_0(x) - \beta_\tau Q^0(x)$ is then equivalent to a deformed harmonic oscillator potential. Although this model has already been used in similar contexts by many authors [6, 14, 36, 37], we discuss it in this Subsection and in Appendix C in some detail, because to our opinion it is highly interesting to see the isovector counterparts of the relations given in the previous Sections, even if those are more model dependent.

In the h.o. model, the bubble graph of Eq.(II.15) assumes a 2-pole form (see Eq.(C.5)), which makes analytic calculations possible. Here, in order to keep the equations as schematic as possible, we restrict ourselves to one h.o. shell ($\Delta N = 0$ space), which corresponds to the first term in Eq.(C.5). (The case of the full h.o. space can be found in Appendix C, and the main points will be summarized in the next Subsection.) In this approximation, where all particle-hole states have the same excitation energy ($e_{0\tau}$), the bubble graph is given by the following one-pole form:

$$\pi_\tau(\omega) = -2\frac{e_{0\tau}}{\omega^2 - e_{0\tau}^2 + i\delta} S_{0\tau}, \qquad \text{(VI.13)}$$

where $e_{0\tau}$ and $S_{0\tau}$ are given by

$$e_{0\tau} = K\beta_\tau, \qquad \left(K = \sqrt{\frac{45}{16\pi}\frac{1}{M\tilde{\omega}}}\right), \qquad \text{(VI.14)}$$

$$S_{0\tau} = \sum_0 |\langle\alpha|Q^1_\tau|i\rangle|^2 = \frac{e^3_{0\tau}}{6\beta^2_\tau} I_\tau = \frac{K^3}{6}\beta_\tau I_\tau. \qquad \text{(VI.15)}$$

The symbol 0 in the sum (VI.15) indicates that only the $\Delta N = 0$ particle-hole states are included, and we used the identity (III.3) and the Inglis formula (III.18) to derive the second equality in (VI.15). The low energy theorem (III.11) relates $S_{0\tau}$ to the quadrupole moment according to[13]

$$S_{0\tau} = \frac{K}{2}\langle Q^0_\tau\rangle_c. \qquad \text{(VI.16)}$$

Using (VI.14) and (VI.16), the self consistency relations (II.6) for the case of exact symmetry ($\varepsilon_\tau = 0$) can be expressed as follows:

$$\begin{aligned} e_{0p} &= -2\chi_{pp}S_{0p} - 2\chi_{pn}S_{0n}, \\ e_{0n} &= -2\chi_{nn}S_{0n} - 2\chi_{np}S_{0p}. \end{aligned} \qquad \text{(VI.17)}$$

Inserting the pole form (VI.13) into the eigenvalue equation (II.16), we get two solutions: The first one is the Goldstone solution ($\omega_0^2 = 0$), and the second one is given by

$$\begin{aligned} \omega_1^2 &= e_{0p}\left(e_{0p} + 2\chi_{pp}S_{0p}\right) + e_{0n}\left(e_{0n} + 2\chi_{nn}S_{0n}\right), \\ &= -2\chi_{pn}\left(e_{0n}S_{0p} + e_{0p}S_{0n}\right) \\ &= -\frac{\chi_{pn}}{3}K^4\,\beta_p\,\beta_n\,I\,. \end{aligned} \qquad \text{(VI.18)}$$

---

[13] As is clear from Eq.(C.5), the $\Delta N = 0$ sum $S_{0\tau}$ is actually only half of the sum in the full h.o. space. This artifact of the restriction to one h.o. shell is formally remedied by replacing the quadrupole moment $\langle Q^0_\tau\rangle$ by the core contribution $\langle Q^0_\tau\rangle_c$, which is half of the total quadrupole moment, in all preceding relations of this paper. See Refs.([6, 30, 33]) for discussions on this point.

Using this solution, it is easy to calculate the proton and neutron normalization factors from Eqs.(II.21), (II.22). The result for the ratio, which corresponds to Eq. (III.14) for the isoscalar Goldstone mode, is

$$\frac{N_n(\omega_1)}{N_p(\omega_1)} = \frac{\omega_1^2 - e_{0n}^2}{\omega_1^2 - e_{0p}^2}\left(-\frac{S_{0p}}{S_{0n}}\right) = -\frac{e_{0n}\chi_{nn} - e_{0p}\chi_{pn}}{e_{0p}\chi_{pp} - e_{0n}\chi_{np}}. \tag{VI.19}$$

The important point to note is that, whereas for the Goldstone mode the ratio N_n/N_p is positive and close to +1, which corresponds to an isoscalar motion, the ratio (VI.19) is negative and close to -1, which corresponds to an isovector motion. For the individual normalization factors we obtain (cf. Eq.(III.19) for the Goldstone mode)

$$N_p(\omega_1) = -\sqrt{\frac{3}{I}}\,\beta_p\sqrt{\frac{I_n}{I_p}}\,\frac{\omega_1^2 - e_{0p}^2}{e_{0p}^2}, \tag{VI.20}$$

$$N_n(\omega_1) = \sqrt{\frac{3}{I}}\,\beta_n\sqrt{\frac{I_p}{I_n}}\,\frac{\omega_1^2 - e_{0n}^2}{e_{0n}^2}. \tag{VI.21}$$

Using these normalization factors and the expression (VI.18) for the excitation energy, it is easy to calculate the RPA amplitudes from (VI.2) and (VI.3). To illustrate the method, which is extended to the full h.o. space in Appendix C, we note that the operator $\mathcal{O}_\tau^\dagger$ of (VI.5) can be expressed as follows:

$$\begin{aligned}\mathcal{O}_\tau^\dagger(\omega_n, K=1) &= -\frac{N_\tau(\omega_n)}{\sqrt{2\omega_n}}\\ &\left[\frac{e_{0\tau}^2}{\omega_n^2 - e_{0\tau}^2 + i\delta}\,\frac{1}{\sqrt{3}\beta_\tau}\,L_\tau^1(0) + \frac{\omega_n}{\omega_n^2 - e_{0\tau}^2 + i\delta}\,Q_\tau^1(0)\right],\end{aligned} \tag{VI.22}$$

where $n = 0, 1$. Here we used the identity (III.3), and defined the "low energy part" of an operator A as follows:

$$A(0) \equiv \sum_0 \left[(A)_{\alpha i}\,a_\alpha^\dagger a_i + (A)_{i\alpha}\,a_i^\dagger a_\alpha\right]. \tag{VI.23}$$

In the $\Delta N = 0$ space, which is considered in this Subsection, we can identify these low energy operators with the full operators ($A(0) \equiv A$). For the Goldstone mode ($\omega_0 = 0$), Eq.(VI.22) reproduces the general result (VI.10), and for the ω_1 mode we obtain

$$\begin{aligned}|\omega_1, K=1\rangle &= \mathcal{O}^\dagger(\omega_1, K=1)|0\rangle\\ &= \left(\mathcal{O}_L^\dagger(\omega_1, K=1) + \mathcal{O}_Q^\dagger(\omega_1, K=1)\right)|0\rangle,\end{aligned} \tag{VI.24}$$

where the creation operator $\mathcal{O}^\dagger$ has been split into an angular momentum part ("L-part") and a quadrupole part ("Q-part") defined by

$$\mathcal{O}_L^\dagger(\omega_1, K=1) = \frac{1}{\sqrt{2\omega_1 I_{IV}}}\left(\frac{2I_n}{I}L_p^1 - \frac{2I_p}{I}L_n^1\right), \tag{VI.25}$$

$$\begin{aligned}&\mathcal{O}_Q^\dagger(\omega_1, K=1)\\ &= \frac{1}{\sqrt{2\omega_1 I_{IV}}}\left(\frac{2I_n}{I}\,\frac{\sqrt{3}\beta_p\omega_1}{e_{0p}^2}\,Q_p^1 - \frac{2I_p}{I}\,\frac{\sqrt{3}\beta_n\omega_1}{e_{0n}^2}\,Q_n^1\right)\\ &= \frac{1}{\sqrt{2\omega_1 I_{IV}}}\sqrt{\frac{-\chi_{pn}I}{\beta_p\beta_n}}\left(\frac{2I_n}{I}\beta_n Q_p^1 - \frac{2I_p}{I}\beta_p Q_n^1\right).\end{aligned} \tag{VI.26}$$

The isovector moment of inertia was defined in (V.15). The L-part (VI.25) has the simple interpretation as the generator of an out of phase rotation of protons against neutrons, where the quantities $2I_n/I$ and $-2I_p/I$ play the role of "effective charges" for protons and neutrons, which effectively remove the contribution of the overall in-phase rotation. The mode which is generated by this operator is therefore called properly the "scissors mode". The Q-part (VI.26), on the other hand, generates the quadrupole vibrations, and we will see below that it gives rise to the restoring force. (More general forms of those generators are given in Appendix C.)

Including also the annihilation operators and the $K = -1$ mode, we can summarize as follows:

$$\begin{aligned}\mathcal{O}^\dagger(\omega_1, K=1) &= \mathcal{O}_L^\dagger(\omega_1, K=1) + \mathcal{O}_Q^\dagger(\omega_1, K=1),\\ \mathcal{O}(\omega_1, K=1) &= \mathcal{O}_L(\omega_1, K=1) + \mathcal{O}_Q(\omega_1, K=1),\\ \mathcal{O}^\dagger(\omega_1, K=-1) &= \mathcal{O}_L(\omega_1, K=1) - \mathcal{O}_Q(\omega_1, K=1),\\ \mathcal{O}(\omega_1, K=-1) &= \mathcal{O}_L^\dagger(\omega_1, K=1) - \mathcal{O}_Q^\dagger(\omega_1, K=1),\end{aligned} \tag{VI.27}$$

where $\mathcal{O}_L^\dagger(\omega_1, K=1)$ and $\mathcal{O}_Q^\dagger(\omega_1, K=1)$ are given in (VI.25) and (VI.26), and

$$\mathcal{O}_L(\omega_1, K=1) = \frac{1}{\sqrt{2\omega_1 I_{IV}}}\left(\frac{2I_n}{I}L_p^{-1} - \frac{2I_p}{I}L_n^{-1}\right), \tag{VI.28}$$

$$\begin{aligned}&\mathcal{O}_Q(\omega_1, K=1) =\\ &-\frac{1}{\sqrt{2\omega_1 I_{IV}}}\sqrt{\frac{-\chi_{pn}I}{\beta_p\beta_n}}\left(\frac{2I_n}{I}\beta_n Q_p^{-1} - \frac{2I_p}{I}\beta_p Q_n^{-1}\right).\end{aligned} \tag{VI.29}$$

By adding the $K = 1$ and $K = -1$ contributions together, it is then easy to calculate the contribution of the ω_1 mode to the effective Hamiltonian (VI.7). We obtain the following result:

$$H_{\text{eff}}(\omega_1) = H_{\text{rot}}(\omega_1) + H_Q(\omega_1), \tag{VI.30}$$

where the rotational and quadrupole vibrational parts are given by

$$
\begin{aligned}
H_{\mathrm{rot}}(\omega_1) &= \omega_1 \left[\mathcal{O}_L^\dagger(\omega_1, K=1)\mathcal{O}_L(\omega_1, K=1) + \mathcal{O}_L(\omega_1, K=1)\mathcal{O}_L^\dagger(\omega_1, K=1)\right], \\
&= \frac{1}{2I}\left[\frac{I_n}{I_p}\left((L_p^x)^2 + (L_p^y)^2\right) + \frac{I_p}{I_n}\left((L_n^x)^2 + (L_n^y)^2\right) - 2\left(L_p^x L_n^x + L_p^y L_n^y\right)\right], \qquad \text{(VI.31)} \\
H_Q(\omega_1) &= \omega_1 \left[\mathcal{O}_Q^\dagger(\omega_1, K=1)\mathcal{O}_Q(\omega_1, K=1) + \mathcal{O}_Q(\omega_1, K=1)\mathcal{O}_Q^\dagger(\omega_1, K=1)\right], \\
&= -\frac{\chi_{pn} I^2}{4\beta_p\beta_n I_p I_n}\left(\frac{2I_n}{I}\beta_n Q_p^1 - \frac{2I_p}{I}\beta_p Q_n^1\right)^\dagger \left(\frac{2I_n}{I}\beta_n Q_p^1 - \frac{2I_p}{I}\beta_p Q_n^1\right). \qquad \text{(VI.32)}
\end{aligned}
$$

By adding (VI.12) and (VI.30), we obtain the total contribution of the isoscalar and isovector rotational states to the effective Hamiltonian:

$$
H_{\mathrm{eff}}(\omega_0) + H_{\mathrm{eff}}(\omega_1) = H_{\mathrm{rot}} + H_Q, \qquad \text{(VI.33)}
$$

where $H_Q = H_Q(\omega_1)$ is given by (VI.32), and H_{rot} by the sum of (VI.12) and (VI.31):

$$
\begin{aligned}
H_{\mathrm{rot}} &= H_{\mathrm{rot}}(\omega_0) + H_{\mathrm{rot}}(\omega_1) \\
&= \frac{(L_p^x)^2 + (L_p^y)^2}{2I_p} + \frac{(L_n^x)^2 + (L_n^y)^2}{2I_n}. \qquad \text{(VI.34)}
\end{aligned}
$$

This is the kinetic part of the 2-rotor model Hamiltonian [11]. We therefore obtain the important result that the 2-rotor model is obtained from the RPA in a natural way by adding the effective Hamiltonians for the Goldstone modes (isoscalar rotation) and the scissors modes (isovector rotation).

We note that the two parts of the effective rotational Hamiltonian, given by the isoscalar Goldstone part (VI.12) and the isovector scissors part (VI.31), correspond exactly to the isoscalar and isovector parts of the M1 operator (V.14). In the notation of first quantization, this is seen most easily by making a minimal substitution, namely $\vec{p}_i \to \vec{p}_i - g_{\ell p}\vec{A}(\vec{r}_i)$ for protons ($i = 1, \ldots Z$) and $\vec{p}_j \to \vec{p}_j - g_{\ell n}\vec{A}(\vec{r}_j)$ for neutrons ($j = 1, \ldots N$), in (VI.12) and (VI.31) separately. Using the form $\vec{A}(\vec{r}_k) = \frac{1}{2}\left(\vec{B} \times \vec{r}_k\right)$, which corresponds to a constant external magnetic field, and expressing the magnetic interaction Hamiltonian in the form $-\vec{B} \cdot \vec{M}/(2M) \equiv -(B^x M^x + B^y M^y)/(2M)$, gives the two terms in (V.14). Viewed in this way, the presence of the scissors part (VI.31) is necessary to give the correct coupling to an external magnetic field.

The quadrupole vibrational part (VI.32) of the effective Hamiltonian is positive definite (note that $\chi_{pn} < 0$), and represents the restoring force which acts against the proton-neutron oscillations in the present model. We note, however, that it cannot be reduced to a simple geometric form, which is usually assumed in the 2-rotor model.

C. Discussions

In the previous Subsection, we have seen how the low-energy isovector scissors modes emerge in the simple approximation of one major h.o. shell ($\Delta N = 0$). The case of the full h.o. space is discussed in detail in Appendix C, and we can summarize the results as follows: There are four solutions of the RPA equation, two at low energy corresponding to the $\Delta N = 0$ case discussed above, and two at high energy ($\Delta N = 2$). Each of these four modes can be represented similar to Eq.(VI.24) by an L-part and a Q-part, as shown in Eq.(C.19). However, the L-part now includes also the generator of quadrupole deformations, describing irrotational flow, in addition to the generator of rotations, as shown by Eqs.(C.23) and (C.24), and the vibrational Q-part includes also the quadrupole operator in p-space in addition to the ordinary one in r-space, as shown by Eqs.(C.25) and (C.26). Concerning the L-part, for not too large deformations, the ordinary rotational term is dominant for the low-energy solutions, while the irrotational term is dominant for the high-energy solutions, as we explain in the last paragraph of Appendix C.

Further information on the nature of these four collective states can be obtained by considering their vertex functions and M1 and E2 transition matrix elements[14], and one arrives at the following picture: One of the high-energy solutions (ω_2 in Appendix C) carries zero M1 strength, and is mainly of irrotational character. It can be identified as the $K = 1$ component of the isoscalar giant quadrupole resonance. The other high-energy solution (ω_3) carries both M1 and E2 strength, and is also mainly of irrotational character. It is usually called the the high-energy scissors mode, or equivalently the $K = 1$ component of the isovector giant quadrupole resonance[19]. The nature of the low-energy solutions is essentially the same as we discussed in the previous Subsections, namely one is the isoscalar rotational mode (ω_0), and the other is the low-energy scissors mode (ω_1), which is mainly of rotational character.

It is very interesting to note that this picture of rotational flow at low energy and irrotational flow at high energy is valid also for other many-body systems, like deformed metallic clusters [38], deformed quantum dots [39], crystals [40], and trapped Bose-Einstein condensates

[41]. (The recent developments are reviewed in Ref.[19].) For example, in the case of deformed metallic clusters, the rotational flow corresponds to a rotation of electrons with respect to the jellium background, and the irrotational flow to a rotation of electrons within a rigid surface. In the case of trapped Bose-Einstein condensates, the collective modes are induced by an abrupt rotation of the deformed trap by a small angle, causing oscillations of the condensed atoms. This case is particularly interesting, because for normal (non-superfluid) gases one expects both the low-energy rotational and high-energy irrotational modes, while for the superfluid case one expects only the high-energy irrotational mode because of the small moment of inertia. Experimental evidence that the low-energy rotational mode of trapped condensed gases indeed exists only above a critical temperature has been reported in Ref.[42].

VII. SUMMARY AND OUTLOOK

In this paper we used a simple field theory model based on a separable QQ interaction to gain analytic insights into the physics of rotational modes in deformed nuclei. Our essential tools were the Ward-Takahashi identities for angular momentum conservation, which we used to discuss the Goldstone modes associated with the spontaneous breaking of rotational symmetry, in particular their vertex functions and decompositions into particle-hole components. In this simple model it was possible to derive analytically the ground state rotational band from the effective Hamiltonian for the isoscalar rotational modes. The isovector rotational (scissors) modes, on the other hand, correspond to a finite intrinsic excitation energy, and their properties depend on the mean field and the residual proton-neutron interaction. In order to obtain analytic results also for the isovector modes, we made use of the harmonic oscillator model for the spherical part of the mean field. It was then possible to derive the vertex functions, the decompositions into particle-hole components, and the effective Hamiltonian also for the scissors modes. By adding the effective Hamiltonians for the Goldstone and the scissors modes, we obtained the kinetic part of the 2-rotor model Hamiltonian, and also the potential energy (restoring force).

An other important part of our analysis was the derivation of the inverse energy weighted and the energy weighted M1 sum rules in the RPA, where we obtained analytic results without resorting to the harmonic oscillator approximation. We discussed those results in connection to recent experimental analysis on the scissors modes. We pointed out that other types of correlations, which are not included in the RPA (for example tensor correlations and meson exchange currents) should enhance the M1 sum rules, because those processes are known to enhance the isovector orbital g-factor. We pointed out an interesting problem in this connection: The experimental data for the inverse energy weighted sum rule seem to require that the isovector and isoscalar orbital g-factors are the same, while observations and theoretical calculations of magnetic moments clearly indicate that the isovector orbital g-factor should be larger than the isoscalar one. It is, however, necessary first to take into account the effects of pairing, and extend the model to include the spin of the nucleons, before one can arrive at firm conclusions.

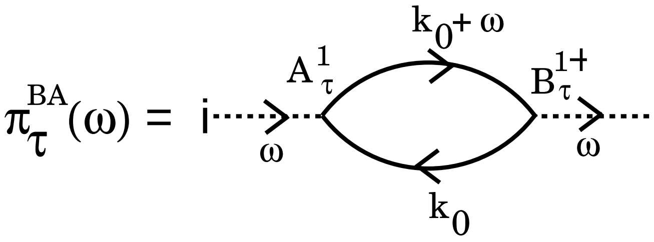

FIG. 9: Graphical representation of the bubble graph $\pi_\tau^{BA}(\omega)$.

We finally mention that some parts of our analytic derivations should be possible for more general interactions, including spin-dependent and non-separable ones. The Ward-Takahashi identities should give an important guide for this purpose.

ACKNOWLEDGMENTS
This work was supported through the Sonderforschungsbereich 634 of the DFG started during an extended visit of one of the authors (W.B.) at the Institute of Nuclear Physics of the TU Darmstadt. He furthermore expresses his thanks to Profs. P. Ring, J. Speth, K. Sugawara-Tanabe, P. Van Isacker, and K. Yazaki for very helpful discussions.

Appendix A: Form of bubble graphs

In this Appendix we give the forms of various bubble graphs which appear in the main text.

We represent a bubble graph $\pi_\tau^{BA}(\omega)$ with external operators $B^{1\dagger}$ and A^1 by Fig.9. (We consider the case where these operators are the spherical $K=1$ components of some tensor operators, since this is actually used in the main text.)

Using the form (II.11) of the propagators and performing the integration over k_0 by residues, we get (see Eq.(II.15) for the special case $A=B=Q$)

$$\pi_\tau^{BA}(\omega) = -\sum_{(\alpha i)\in\tau}\left[\frac{\langle\alpha|A^1|i\rangle\langle\alpha|B^1|i\rangle^*}{\omega-\omega_{\alpha i}+i\delta} - \frac{\langle i|A^1|\alpha\rangle\langle i|B^1|\alpha\rangle^*}{\omega+\omega_{\alpha i}-i\delta}\right]. \tag{A.1}$$

In order to combine these two terms, one changes the sum over the single particle states (αi) in the second term to the time reversed states $(\overline{\alpha i})$, which have the opposite values of ℓ_z but the same energies for the axial symmetric case. Then one uses the property (see Eq.(A.22) of [1])

$$\langle \bar{i}|\mathcal{O}|\bar{\alpha}\rangle = t_{\mathcal{O}}\langle\alpha|\mathcal{O}|i\rangle, \tag{A.2}$$

where $t_{\mathcal{O}} = +1$ for a T-even operator (like the quadrupole operator in our case), and $t_{\mathcal{O}} = -1$ for a T-odd operator (like the angular momentum operator in our case). As a result, the relative sign of the forward and backward terms is different for the cases where both operators have the same or the opposite T-symmetry, and one obtains

$$\pi_\tau^{BA}(\omega) = -2\sum_{(\alpha i)\in\tau}\langle\alpha|A^1|i\rangle\langle\alpha|B^1|i\rangle^*\frac{\Omega}{\omega^2-\omega_{\alpha i}^2+i\delta}, \tag{A.3}$$

where $\Omega = \omega_{\alpha i}$ if $t_A = t_B$, and $\Omega = \omega$ if $t_A = -t_B$.

For the cases needed in the main text, the bubble graphs are then obtained as follows:

$$\pi_\tau^{QQ}(\omega) \equiv \pi_\tau(\omega) = -2\sum_{(\alpha i)\in\tau}|\langle\alpha|Q^1|i\rangle|^2\frac{\omega_{\alpha i}}{\omega^2-\omega_{\alpha i}^2+i\delta}, \tag{A.4}$$

$$\begin{aligned}\pi_\tau^{QL}(\omega) &= -2\omega\sum_{(\alpha i)\in\tau}\langle\alpha|L^1|i\rangle\langle\alpha|Q^1|i\rangle^*\frac{1}{\omega^2-\omega_{\alpha i}^2+i\delta},\\ &= -2\omega\sum_{(\alpha i)\in\tau}\langle\alpha|L^{-1}|i\rangle^*\langle\alpha|Q^{-1}|i\rangle\frac{1}{\omega^2-\omega_{\alpha i}^2+i\delta},\end{aligned} \tag{A.5}$$

$$\pi_\tau^{LL}(\omega) = -2\sum_{(\alpha i)\in\tau}|\langle\alpha|L^1|i\rangle|^2\frac{\omega_{\alpha i}}{\omega^2-\omega_{\alpha i}^2+i\delta}. \tag{A.6}$$

The two identical forms of the mixed bubble graph in (A.5) are obtained by expressing either the first or the second term in (A.1) by the time reversed states $(\overline{\alpha i})$. We also note that all bubble graphs which appear in this paper correspond to $K = 1$, although this is not indicated explicitly in our notations.

Appendix B: Identities for bubble graphs

In this Appendix we use the forms of the bubble graphs given in Appendix A to confirm various identities which are derived more generally in the main text.

1. Eq.(III.11)

We use Eq.(A.4) and the identity (III.3) to write

$$\begin{aligned}\pi_\tau(0) &= 2\sum_{(PH)\in\tau}\frac{|\langle PH|Q^1|0\rangle|^2}{\omega_{PH}}\\ &= \frac{2}{3\beta_\tau^2}\sum_{(PH)\in\tau}\omega_{PH}|\langle PH|L^1|0\rangle|^2,\end{aligned} \tag{B.1}$$

where only in this and the following equation we denote the non-interacting (mean field) ground state simply by $|0\rangle$, the non-interacting particle-hole states by $|PH\rangle$, and their energies by ω_{PH}. Since (B.1) has the form of an energy weighted sum rule, it can be expressed as a double commutator in the standard way, and we obtain

$$\begin{aligned}\beta_\tau\pi_\tau(0) &= -\frac{1}{3\beta_\tau}\langle 0|\left[\left[H_0, L_\tau^1\right], L_\tau^{-1}\right]|0\rangle,\\ &= -\frac{1}{\sqrt{3}}\langle 0|\left[Q_\tau^1, L_\tau^{\bar{1}}\right]|0\rangle = \langle 0|Q_\tau^0|0\rangle,\end{aligned} \tag{B.2}$$

where in the last two steps we used the commutation relations (III.1) and (III.2).

2. Eq.(III.23)

If we insert the identity (III.3) into the first form (A.5) of π_τ^{QL} and compare the result to the form (A.4) of π_τ^{QQ} we obtain the following identity:

$$\omega\pi_\tau^{QL}(\omega) = \sqrt{3}\beta_\tau\left(\pi_\tau(\omega) - \pi_\tau(0)\right). \tag{B.3}$$

Then, in order to show Eq.(III.23), we have to show that the following relation holds if $\omega = \omega_n$ is a solution of the eigenvalue equation (II.16):

$$\left(\pi_p(\omega) - \pi_p(0)\right) + \frac{N_n(\omega)}{N_p(\omega)}\frac{\beta_n}{\beta_p}\left(\pi_n(\omega) - \pi_n(0)\right) = 0. \tag{B.4}$$

Here the ratio of the normalization factors is given by (II.22), and the ratio of deformation parameters by (III.14). Using these relations, we can express (B.4) solely by bubble graphs as follows:

$$\begin{aligned}&\left(\pi_p(\omega) - \pi_p(0)\right)\\ &+ \frac{\left(1+\chi_{pp}\pi_p(\omega)\right)\pi_p(0)}{\left(1+\chi_{nn}\pi_n(0)\right)\pi_n(\omega)}\left(\pi_n(\omega) - \pi_n(0)\right) = 0.\end{aligned} \tag{B.5}$$

More explicitly, the relation (B.5) can be written as

$$\begin{aligned}&\pi_p(\omega)\pi_n(\omega) - \pi_p(0)\pi_n(0)\\ &+ \chi_{pp}\Big[\pi_p(\omega)\pi_n(\omega)\pi_p(0) + \pi_p(\omega)\pi_n(\omega)\pi_n(0)\\ &\qquad - \pi_p(\omega)\pi_p(0)\pi_n(0) - \pi_n(\omega)\pi_p(0)\pi_n(0)\Big] = 0.\end{aligned} \tag{B.6}$$

In order to verify this relation, we use the eigenvalue equation (II.16) for $\omega = \omega_n$ as well as for $\omega = 0$. (Note that for $\omega = 0$ the RPA equation is equivalent to the self consistency relation, as we have shown in the main text.) This gives the following identity:

$$\frac{\left(1+\chi_{pp}\pi_p(\omega)\right)\left(1+\chi_{nn}\pi_n(\omega)\right)}{\left(1+\chi_{pp}\pi_p(0)\right)\left(1+\chi_{nn}\pi_n(0)\right)} = \frac{\pi_p(\omega)\pi_n(\omega)}{\pi_p(0)\pi_n(0)}. \tag{B.7}$$

It is readily seen that this relation is the same as (B.6). This concludes the explicit verification of Eq.(III.23).

3. Eqs.(III.26) and (III.27)

Using Eq.(A.5) for the bubble graph π_τ^{QL} and the identity (III.3) we obtain

$$\lim_{\omega\to 0}\left(\frac{\pi_\tau^{QL}(\omega)}{\omega}\right) = \frac{2}{\sqrt{3}\beta_\tau}\sum_{(\alpha i)\in\tau}\frac{|\langle\alpha|L^1|i\rangle|^2}{\omega_{\alpha i}}.$$

Using then the Inglis formula (III.18) we obtain (III.27).

Appendix C: Deformed harmonic oscillator

In this Appendix we review some formulas [6, 10, 14, 36, 37] for the RPA calculation with deformed h.o. mean fields.

Using $U_0(x) = M\tilde{\omega}^2 r^2/2$ in the mean field Hamiltonian (II.4), the sum $U_0(x) - \beta_\tau Q^0(x)$ becomes a deformed h.o. potential with frequencies

$$\begin{aligned} \tilde{\omega}_{x,\tau} &= \tilde{\omega}_{y,\tau} = \tilde{\omega}\sqrt{1+\frac{2}{3}\delta_\tau}, \\ \tilde{\omega}_{z,\tau} &= \tilde{\omega}\sqrt{1-\frac{4}{3}\delta_\tau}, \end{aligned} \tag{C.1}$$

where the dimensionless deformation parameters δ_τ are related to the β_τ of the main text by

$$\delta_\tau = \frac{K}{\tilde{\omega}}\beta_\tau, \tag{C.2}$$

and K is defined in Eq.(VI.14). In this simple model, two types of particle-hole excitations contribute to the bubble graph of Eq.(II.15), corresponding to excitations within one h.o. shell ($\Delta N = 0$) and across two shells ($\Delta N = 2$). The corresponding excitation energies are given by

$$e_{0\tau} = \tilde{\omega}_{x,\tau} - \tilde{\omega}_{z,\tau} \simeq \delta_\tau\,\tilde{\omega}\,, \tag{C.3}$$

$$e_{2\tau} = \tilde{\omega}_{x,\tau} + \tilde{\omega}_{z,\tau} \simeq 2\tilde{\omega}\left(1-\frac{1}{6}\delta_\tau\right). \tag{C.4}$$

The bubble graph (II.15) then takes the form

$$\begin{aligned} \pi_\tau(\omega) &= -2\left(\frac{e_{0\tau}}{\omega^2-e_{0\tau}^2}S_{0\tau} + \frac{e_{2\tau}}{\omega^2-e_{2\tau}^2}S_{2\tau}\right), \\ &= -2\left(\frac{e_{0\tau}^2}{\omega^2-e_{0\tau}^2} + \frac{e_{2\tau}^2}{\omega^2-e_{2\tau}^2}\right)\frac{S_{0\tau}}{e_{0\tau}}. \end{aligned} \tag{C.5}$$

Here the quantities

$$S_{0\tau} = \sum_0 |\langle\alpha|Q_\tau^1|i\rangle|^2, \qquad S_{2\tau} = \sum_2 |\langle\alpha|Q_\tau^1|i\rangle|^2, \tag{C.6}$$

denote the sums over the $\Delta N = 0$ and $\Delta N = 2$ particle-hole states, and in the second equality of (C.5) we used the relation[6]

$$\frac{S_{0\tau}}{e_{0\tau}} = \frac{S_{2\tau}}{e_{2\tau}}. \tag{C.7}$$

This relation, which follows from the analytic forms of $S_{0\tau}$ and $S_{2\tau}$ given by Eq.(27) of Ref.[36], shows that the $\Delta N = 0$ and $\Delta N = 2$ excitations give the same contributions to $\pi_\tau(0)$. The low energy theorem (III.11) then can be written in the form

$$S_{0\tau} = \frac{K}{4}\langle Q_\tau^0\rangle. \tag{C.8}$$

Using (C.3) and (C.8), the self consistency relations (II.6) take the form

$$e_{0p} = -4\chi_{pp}\,S_{0p} - 4\chi_{pn}\,S_{0n}, \tag{C.9}$$

$$e_{0n} = -4\chi_{nn}\,S_{0n} - 4\chi_{np}\,S_{0p}. \tag{C.10}$$

Inserting the form (C.5) of the bubble graph into the eigenvalue equation (II.16), we can calculate the collective excitation energies in this model. Besides the Goldstone solution ($\omega_0 = 0$), there are three solutions ($\omega_1, \omega_2, \omega_3$) with positive energy, which are determined by the following cubic equation[6] in $x \equiv \omega^2$:

$$x^3 - ax^2 + bx - c = 0, \tag{C.11}$$

with the coefficients

$$a = \left(e_{0p}^2 + e_{2p}^2\right)W_p(2) + (p\to n), \tag{C.12}$$

$$\begin{aligned} b &= e_{0p}^2 e_{2p}^2 W_p(4) + (p\to n) \\ &+ \frac{1}{4}\left(e_{0p}^2+e_{2p}^2\right)\left(e_{0n}^2+e_{2n}^2\right)\left(1+W_p(4)+W_n(4)\right), \end{aligned} \tag{C.13}$$

$$c = \frac{1}{2}e_{0p}^2 e_{2p}^2\left(e_{0n}^2+e_{2n}^2\right)W_p(4) + (p\to n). \tag{C.14}$$

Here we defined (for $k = 2, 4$)

$$W_\tau(k) = 1 + k\frac{\chi_{pp}}{e_{0\tau}}S_{0\tau}.$$

For the case where the proton and neutron deformations can be assumed to be equal ($\delta_p = \delta_n$, which implies $e_{0p} = e_{0n} \equiv e_0$ and $e_{2p} = e_{2n} \equiv e_2$), simple analytic solutions of (C.11) exist: One can be obtained by noting that for

$$\omega_2 = \sqrt{\frac{e_0^2+e_2^2}{2}} = \sqrt{\tilde{\omega}_x^2+\tilde{\omega}_z^2} \tag{C.15}$$

the bubble graph (C.5) has the same value as for $\omega_0 = 0$. Since $\omega_0 = 0$ is a solution of the eigenvalue equation because of the self consistence relations, (C.15) is also a solution. To further understand the physical nature of this solution, we note that because of $\pi(\omega_2) = \pi(0)$, the identity (B.3) shows that $\pi^{QL}(\omega_2) = 0$, i.e., the M1 transition matrix element ($B(M1)$ of (IV.1)) vanishes for this mode. On the other hand, $B(E2)$ is non-zero[14], and this mode can therefore be identified as the $K = 1$ component of the isoscalar giant quadrupole resonance [14]. The remaining two solutions can then be found by solving simple quadratic equations. One obtains to lowest order in δ:

$$\omega_1 = e_0\sqrt{1+\frac{b}{2+b}}, \tag{C.16}$$

$$\omega_3 = e_2\sqrt{1+\frac{b}{2}}, \tag{C.17}$$

where

$$b = -\frac{\chi_{pp}-\chi_{pn}}{\chi_{pp}+\chi_{pn}} = -\frac{\chi(T=1)}{\chi(T=0)} \tag{C.18}$$

is the ratio of the isovector to the isoscalar interaction strength ($b>0$). Analytic solutions can be worked out also for the case of different proton and neutron deformation parameters, although the expressions become quite long. To summarize, there are four solutions of the RPA equation, where ω_0, ω_1 are the "low-energy" solutions, and ω_2, ω_3 the "high-energy" solutions. For each solution, one can determine the normalization factors $N_p(\omega_n)$ and $N_n(\omega_n)$ from (II.21) and (II.22).

Let us outline here the calculation of the creation operator (VI.5) for any of these modes, following the method explained in Refs.[10, 36] [14]: If we add the contribution of the $\Delta N = 2$ excitations to Eq.(VI.22) of the main text, we obtain

$$\begin{aligned}\mathcal{O}^\dagger(\omega_n,K=1) &= -\frac{N(\omega_n)}{\sqrt{2\omega_n}} \\ &\sum_{m=0,2}\left[\frac{e_m^2}{\omega_n^2-e_m^2}\frac{1}{\sqrt{3}\beta}\,L^1(m)+\frac{\omega_n}{\omega_n^2-e_m^2}\,Q^1(m)\right], \\ &\equiv \mathcal{O}_L^\dagger(\omega_n,K=1)+\mathcal{O}_Q^\dagger(\omega_n,K=1).\end{aligned} \tag{C.19}$$

Here $\omega_0,\dots\omega_3$ denote the RPA eigenvalues, and in addition to the "low energy part" of an operator A, which was defined in (VI.23) of the main text, we also define the "high energy part" as

$$A(2) = \sum_2\left[(A)_{\alpha i}\,a_\alpha^\dagger a_i + (A)_{i\alpha}\,a_i^\dagger a_\alpha\right]. \tag{C.20}$$

In the harmonic oscillator model, explicit forms of the operators $L^1(m)$ and $Q^1(m)$, where $m = 0,2$, can be derived as follows: We have

$$L^1 = -i\sum_j\left[(x+iy)_j\,p_{zj} - (p_x+ip_y)_j\,z_j\right], \tag{C.21}$$

$$Q^1 = -\sqrt{\frac{15}{8\pi}}\sum_j z_j\,(x+iy)_j\,, \tag{C.22}$$

where j labels the nucleons. If we express (C.21) and (C.22) in terms of the standard creation and annihilation operators $a_k^\dagger$ and a_k ($k = x,y,z$) for each particle, we obtain two kinds of terms: The first kind involves products $a_z^\dagger a_i$ and $a_i^\dagger a_z$ with $i = x,y$, and the second kind involved products $a_z^\dagger a_i^\dagger$ and $a_z a_i$. It is clear that the first kind of operators contributes exclusively to $\Delta N = 0$ excitations (operators $A(0)$), and the second one exclusively to $\Delta N = 2$ excitations (operators $A(2)$). Then, for each part $A(m)$ separately, one can reexpresses the creation and annihilation operators by the original position and momentum operators. In this way one obtains the decompositions $L^1 = L^1(0) + L^1(2)$ and $Q^1 = Q^1(0) + Q^1(2)$, where

$$\begin{aligned}L^1(0) &= \frac{(\tilde\omega_x+\tilde\omega_z)^2}{4\tilde\omega_x\tilde\omega_z}\left\{L^1 - i\,\frac{\tilde\omega_x-\tilde\omega_z}{\tilde\omega_x+\tilde\omega_z}\sum_j\left[(x+iy)_j\,p_{zj}+(p_x+ip_y)_j\,z_j\right]\right\}, \\ &= \frac{(\tilde\omega_x+\tilde\omega_z)^2}{4\tilde\omega_x\tilde\omega_z}\,2i\sum_j\left\{\left[r_j^{(1)}\times p_j^{(1)}\right]^1_{(1)}+\frac{\tilde\omega_x-\tilde\omega_z}{\tilde\omega_x+\tilde\omega_z}\left[r_j^{(1)}\times p_j^{(1)}\right]^1_{(2)}\right\},\end{aligned} \tag{C.23}$$

$$\begin{aligned}L^1(2) &= -\frac{(\tilde\omega_x-\tilde\omega_z)^2}{4\tilde\omega_x\tilde\omega_z}\left\{L^1 - i\frac{\tilde\omega_x+\tilde\omega_z}{\tilde\omega_x-\tilde\omega_z}\sum_j\left[(x+iy)_j\,p_{zj}+(p_x+ip_y)_j\,z_j\right]\right\}, \\ &= -\frac{(\tilde\omega_x-\tilde\omega_z)^2}{4\tilde\omega_x\tilde\omega_z}\,2i\sum_j\left\{\left[r_j^{(1)}\times p_j^{(1)}\right]^1_{(1)}+\frac{\tilde\omega_x+\tilde\omega_z}{\tilde\omega_x-\tilde\omega_z}\left[r_j^{(1)}\times p_j^{(1)}\right]^1_{(2)}\right\},\end{aligned} \tag{C.24}$$

---

[14] For simplicity, we write the following expressions in first quantization and omit the distinction between protons and neutrons.

and

$$Q^1(0) = \frac{1}{2}Q^1 - \sqrt{\frac{15}{8\pi}}\,\frac{1}{2M^2\tilde{\omega}_x\tilde{\omega}_z}\sum_j p_{zj}\left(p_x + ip_y\right)_j = \sqrt{\frac{15}{8\pi}}\,\frac{1}{2}\sum_j\left\{\left[r_j^{(1)}\times r_j^{(1)}\right]^1_{(2)} + \frac{1}{M^2\tilde{\omega}_x\tilde{\omega}_z}\left[p_j^{(1)}\times p_j^{(1)}\right]^1_{(2)}\right\}, \tag{C.25}$$

$$Q^1(2) = \frac{1}{2}Q^1 + \sqrt{\frac{15}{8\pi}}\,\frac{1}{2M^2\tilde{\omega}_x\tilde{\omega}_z}\sum_j p_{zj}\left(p_x + ip_y\right)_j = \sqrt{\frac{15}{8\pi}}\,\frac{1}{2}\sum_j\left\{\left[r_j^{(1)}\times r_j^{(1)}\right]^1_{(2)} - \frac{1}{M^2\tilde{\omega}_x\tilde{\omega}_z}\left[p_j^{(1)}\times p_j^{(1)}\right]^1_{(2)}\right\}. \tag{C.26}$$

Here $\left[a^{(1)}\times b^{(1)}\right]^q_{(k)}$ denotes the tensor product, with rank k and spherical component q, of two vectors $\vec{a}$ and $\vec{b}$, according to the definitions of Ref.[26]. The forms given above exhaust all possible one-particle tensor operators which can be formed from the position and momentum operators.

Inserting these forms into (C.19), we arrive at the final expression for the creation operator of each mode. We also note that the relations (VI.27) of the main text are still valid with the above extended operators, and therefore also the expressions given in the first lines of Eq.(VI.31) and (VI.32) remain valid.

We see that, in addition to the two operators L^1 and Q^1, the presence of the high energy modes leads to two more types of operators, namely $\left[r^{(1)}\times p^{(1)}\right]^1_{(2)}$ and $\left[p^{(1)}\times p^{(1)}\right]^1_{(2)}$. In particular, the operator $\left[r^{(1)}\times p^{(1)}\right]^1_{(2)}$ is the generator of quadrupole deformations[10], and describes irrotational flow. This is easily seen by noting that, for example, the part in $\{\dots\}$ in the first line of Eq.(C.23), which corresponds to the motion around the x axis, is given by $\sum_j\left[\left(yp_z - zp_y\right)_j + \frac{\delta}{2}\left(yp_z + zp_y\right)_j\right]$. It generates the displacement $\propto\left(\vec{e}_x\times\vec{r} + \frac{\delta}{2}\vec{\nabla}yz\right)$ of the volume element of the liquid, which consists of a rotational and irrotational part. We also note that, in contrast to the angular momentum, the generator of quadrupole deformations is not a symmetry transformation of the Hamiltonian.

For not too large deformation, we see from (C.23) and (C.24) that the rotational term is dominant in the low-energy part $L^1(0)$, and the irrotational term is dominant in the high-energy part $L^1(2)$. Going back to Eq.(C.19), this implies that the low enery solutions correspond mainly to rotational flow, and the high energy solutions mainly to irrotational flow. Further information on the character of these modes is obtained by considering their vertex functions and M1 and E2 transition matrix elements[14], which leads to the following picture: The ω_0 mode is the isoscalar rotational (intrinsic Goldstone) mode, and the ω_2 mode is the $K = 1$ component of the isoscalar giant quadrupole resonance, as noted already above. The remaining modes ω_1 and ω_3 are of isovector type, and carry both M1 and E2 strength. The ω_1 mode is mainly of rotational nature and is called the low-energy scissors mode, while the ω_3 mode is mainly of irrotational nature and is called the high-energy scissors mode or, equivalently, the $K = 1$ component of the isovector giant quadrupole resonance[19].

[1] D.J. Rowe, Nuclear Collective Motion, Methuen and Co., 1970.

[2] P. Ring, and P. Schuck, The Nuclear Many-Body Problem, Springer, 1980.

[3] V.A. Khodel, and E.E. Saperstein, Phys. Rept. **92** (1982) 183.

[4] J.W. Negele, and H. Orland, Quantum Many-Particle Systems, Addison-Weseley, 1988.

[5] H. Ui, and G. Takeda, Prog. Theor. Phys. **70** (1983) 176.

[6] N. Lo Iudice, Nucl. Phys. **A 605** (1996) 61.

[7] K. Fujikawa, and H. Ui, Prog. Theor. Phys. **75** (1986) 997.

[8] T. Papenbrock, Nucl. Phys. **A 852** (2011) 36.

[9] D. Bohle, A. Richter, W. Steffen, A.E.L. Dieperink, N. Lo Iudice, F. Palumbo, and O. Scholten, Phys. Lett. **B 137** (1984) 27.

[10] D. Zawischa, Prog. Nucl. Part. Phys. **24** (1998) 683.

[11] N. Lo Iudice, and F. Palumbo, Phys. Rev. Lett. **41** (1978) 1532.

[12] E. Lipparini, and S. Stringari, Phys. Lett. **B 130** (1983) 139.

[13] O. Scholten, K. Heyde, P. van Isacker, J. Jolie, J. Moreau, M. Waroquier, and J. Sau, Nucl. Phys. **A 438** (1985) 41; T. Mizusaki, T. Otsuka, and M. Sugita, Phys. Rev. **C 44** (1991) R1277.

[14] N. Lo Iudice, Phys. Rev. **C 57** (1998) 1246.

[15] J. Enders, P. von Neumann-Cosel, C. Rangacharyulu, and A. Richter, Phys. Rev. **C 71** (2005) 014306.

[16] J. Enders, H. Kaiser, P. von Neumann-Cosel, C. Rangacharyulu, and A. Richter, Phys. Rev. **C 59** (1999) R1851.

[17] E. Lipparini, and S. Stringari, Phys. Rept. **175** (1989) 103.

[18] D. Zawischa, M. Macfarlane, and J. Speth, Phys. Rev. **C**

42 (1990) 1461.

[19] K. Heyde, P. von Neumann-Cosel, and A. Richter, Rev. Mod. Phys. **82** (2010) 2365.

[20] Y. Takahashi, Nuovo Cim. **6** (1957) 371.

[21] D.R. Bes, and R.A. Broglia, Phys. Lett. **B 137** (1984) 121;
S. Iwasaki, and K. Hara, Phys. Lett. **B 144** (1984) 9;
K. Sugawara-Tanabe, and A. Arima, Phys. Lett. **B 206** (1988) 573; **229** (1989) 327.

[22] I. Hamamoto, and S. Aberg, Phys. Lett. **B 145** (1984) 163;
I. Hamamoto, and C. Magnusson, Phys. Lett. **B 260** (1991) 6.

[23] R. Nojarov, and A. Faessler, Nucl. Phys. **A 484** (1988) 1;
A. Faessler, R. Nojarov, and F.G. Scholtz, Nucl. Phys. **A 515** (1990) 237.

[24] Y. Nambu, Phys. Rev. **117** (1960) 648;
L.P. Gorkov, JETP **7** (1958) 993;
M. Mukerjee, and Y. Nambu, Ann. Phys. **191** (1989) 143.

[25] S.G. Nilsson, Mat. Fys. Medd. Dan. Vid. Selsk. **29** (1955) No. 16.

[26] A. Messiah, Quantum Mechanics (Dover Publications, 1999), Appendix C.

[27] D.R. Inglis, Phys. Rev. **96** (1954) 1059.

[28] A.B. Migdal, *Theory of finite Fermi systems and applications to atomic nuclei*, Wiley, New York, 1967.

[29] A. Arima, K. Shimizu, W. Bentz, and H. Hyuga, Adv. Nucl. Phys. **18** (1987) 1.

[30] E. Moya de Guerra, and L. Zamick, Phys. Rev. **C 47** (1993) 2604.

[31] W. Bentz, and A. Arima, Nucl. Phys. **A 736** (2004) 93.

[32] A. Bohr, and B.R. Mottelson, *Nuclear Structure*, Vol. II (World Scientific, 1998).

[33] D.R. Bes, and R.A. Sorensen, Adv. Nucl. Phys. **2** (1969) 129.

[34] T. Eguchi, Phys. Rev. **D 14** (1976) 2755.

[35] M.B. Barbaro, A. Molinari, F. Palumbo, and M.R. Quaglia, Phys. Rev. **C 70** (2004) 034309;
F. Palumbo, Ann. Phys. **324** (2009) 2226.

[36] T. Suzuki, and D.J. Rowe, Nucl. Phys. **A 289** (1977) 461.

[37] H. Kurasawa, and T. Suzuki, Phys. Lett. **B 144** (1984) 151.

[38] E. Lipparini, and S. Stringari, Phys. Rev. Lett. **63** (1989) 570.

[39] D.G. Austing, S. Sasaki, S. Tarucha, S.M. Reimann, M. Koskinen, and M. Manninen, Phys. Rev. **B 60** (1999) 11514.

[40] K. Hatada, K. Hayakawa, and F. Palumbo, Phys. Rev. **B 71** (2005) 092402.

[41] D. Guéry-Odelin, and S. Stringari, Phys. Rev. Lett. **83** (1999) 4452.

[42] O.M. Maragò, S.A. Hopkins, J. Arlt, E. Hodby, G. Hechenblaikner, and C.J. Foot, Phys. Rev. Lett. **84** (2000) 2056.